Electronic Supplementary Material (ESI) for Food & Function

Supporting information

Characterisation of "caramel-type" thermal decomposition products of selected monosaccharides including fructose, mannose, galactose, arabinose and ribose by advanced electrospray ionization mass spectrometry methods

Agnieszka Golon and Nikolai Kuhnert*

School of Engineering and Science, Jacobs University Bremen,

Campus Ring 1, 28759 Bremen, Germany

To whom correspondence should be addressed. E-mail: n.kuhnert@jacobs-university.de

Table of Contents:

Figure S5 ^{1}H NMR spectra of caramelized a) fructose, b) galactose and c) mannose

Figure S6 EIC at *m/z* 341.0 ($C_{12}H_{22}O_{11}$) for caramelised fructose in the negative ion mode

Figure S7 EIC at *m/z* 341.0 ($C_{12}H_{22}O_{11}$) for caramelised galactose in the negative ion mode

Figure S8 MS^2 spectra of fragment at *m/z* 341.0 ($C_{12}H_{22}O_{11}$) for five chromatographic peaks of caramelised fructose in the negative ion mode

Figure S9 MS^2 spectra of fragment at *m/z* 503.0 ($C_{18}H_{32}O_{16}$) for ten chromatographic peaks of caramelised fructose in the negative ion mode

Figure S10 MS^2 spectra of fragment at *m/z* 647.0 ($C_{24}H_{40}O_{20}$) for ten chromatographic peaks of caramelised fructose in the negative ion mode

Figure S11 MS^2 spectra of fragment at *m/z* 809.0 ($C_{30}H_{50}O_{25}$) for seven chromatographic peaks of caramelised fructose in the negative ion mode

Figure S12 MS^2 spectra of fragment at *m/z* 341.0 ($C_{12}H_{22}O_{11}$) for two chromatographic peaks of caramelised galactose in the negative ion mode

Figure S13 MS^2 spectra of fragment at *m/z* 503.0 ($C_{18}H_{32}O_{16}$) for four chromatographic peaks of caramelised galactose in the negative ion mode

Figure S14 MS^2 spectra of fragment at *m/z* 503.0 ($C_{18}H_{32}O_{16}$) for four chromatographic peaks of caramelised mannose in the negative ion mode

Figure S15 MS^2 spectra of fragment at *m/z* 647.0 ($C_{24}H_{40}O_{20}$) for ten chromatographic peaks of caramelised mannose in the negative ion mode

Figure S16 MS^2 spectra of fragment at *m/z* 809.0 ($C_{30}H_{50}O_{25}$) for seven chromatographic peaks of caramelised mannose in the negative ion mode

Figure S17 EIC at *m/z* 161.0 ($C_6H_{10}O_5$) for caramelised fructose in the negative ion mode

Figure S18 EIC at *m/z* 323.0 ($C_{12}H_{20}O_{10}$) for caramelised fructose in the negative ion mode

Figure S19 EIC at *m/z* 161.0 ($C_6H_{10}O_5$) for caramelised galactose in the negative ion mode

Figure S20 EIC at *m/z* 323.0 ($C_{12}H_{20}O_{10}$) for caramelised galactose in the negative ion mode

Figure S21 EIC at *m/z* 323.0 ($C_{12}H_{20}O_{10}$) for caramelised mannose in the negative ion mode

Figure S22 EIC at *m/z* 359.0 ($C_{12}H_{24}O_{12}$) for caramelised fructose in the negative ion mode

Figure S23 EIC at *m/z* 359.0 ($C_{12}H_{24}O_{12}$) for caramelised galactose in the negative ion mode

Figure S24 EIC at *m/z* 149.0 ($C_5H_{10}O_5$) for caramelised rybose in negative ion mode

Figure S25 MS^2 spectra of fragment at *m/z* 149.0 ($C_5H_{10}O_5$) for three chromatographic peaks of caramelised rybose in the negative ion mode

Figure S26 EIC at *m/z* 149.0 ($C_5H_{10}O_5$) for caramelised arabinose in the negative ion mode

Figure S27 MS^2 spectra of fragment at *m/z* 149 ($C_5H_8O_4$) for three chromatographic peaks of caramelised arabinose in the negative ion mode

Figure S28 EIC at *m/z* 281.0 ($C_{10}H_{18}O_9$) for caramelised rybose in the negative ion mode

Figure S29 MS^2 spectra of fragment at *m/z* 281.0 ($C_{10}H_{18}O_9$) for four chromatographic peaks of caramelised rybose in the negative ion mode

Figure S30 EIC at *m/z* 281.0 ($C_{10}H_{18}O_9$) for caramelised arabinose in the negative ion mode

Figure S31 MS^2 spectra of fragment at *m/z* 281.0 ($C_{10}H_{18}O_9$) for ten chromatographic peaks of caramelised arabinose in the negative ion mode

Figure S32 EIC at *m/z* 413.0 ($C_{15}H_{26}O_{13}$) for caramelised rybose in the negative ion mode

Figure S33 MS^2 spectra of fragment at *m/z* 413.0 ($C_{15}H_{26}O_{13}$) for three chromatographic peaks of caramelised rybose in the negative ion mode

Figure S34 EIC at *m/z* 413.0 ($C_{15}H_{26}O_{13}$) for caramelised arabinose in the negative ion mode

Figure S35 MS^2 spectra of fragment at *m/z* 413.0 ($C_{15}H_{26}O_{13}$) for six chromatographic peaks of caramelised arabinose in the negative ion mode

Figure S36 EIC at *m/z* 113.0 ($C_5H_6O_3$) for caramelised rybose in the negative ion mode

Figure S37 EIC at *m/z* 113.0 ($C_5H_6O_3$) for caramelised arabinose in the negative ion mode

Figure S38 EIC at *m/z* 263.0 ($C_{10}H_{16}O_8$) for caramelised rybose in the negative ion mode

Figure S39 MS^2 spectra of fragment at *m/z* 263.0 ($C_{10}H_{16}O_8$) for seven chromatographic peaks of caramelised rybose in the negative ion mode

Figure S40 EIC at *m/z* 263.0 ($C_{10}H_{16}O_8$) for caramelised arabinose in the negative ion mode

Figure S41 MS^2 spectra of fragment at *m/z* 263 ($C_{10}H_{16}O_8$) for three chromatographic peaks of caramelised arabinose in the negative ion mode

Figure S42 EIC at *m/z* 395.0 ($C_{15}H_{24}O_{12}$) for caramelised arabinose in the negative ion mode

Figure S43 MS^2 spectra of fragment at *m/z* 395.0 ($C_{15}H_{24}O_{12}$) for six chromatographic peaks of caramelised arabinose in the negative ion mode

Figure S44 EIC at *m/z* 527.0 ($C_{20}H_{32}O_{16}$) for caramelised rybose in the negative ion mode

Figure S45 MS^2 spectra of fragment at *m/z* 527.0 ($C_{20}H_{32}O_{16}$) for six chromatographic peaks of caramelised rybose in the negative ion mode

Figure S46 EIC at *m/z* 791.0 ($C_{30}H_{48}O_{24}$) for caramelised rybose in the negative ion mode

Figure S47 MS^2 spectra of fragment at *m/z* 791.0 ($C_{30}H_{48}O_{24}$) for six chromatographic peaks of caramelised rybose in the negative ion mode

TableS2 Negative ion mode ESI-MS/MS data for caramelised fructose

TableS3 Negative ion mode ESI-MS/MS data for caramelised galactose

TableS4 Negative ion mode ESI-MS/MS data for caramelised mannose

a)

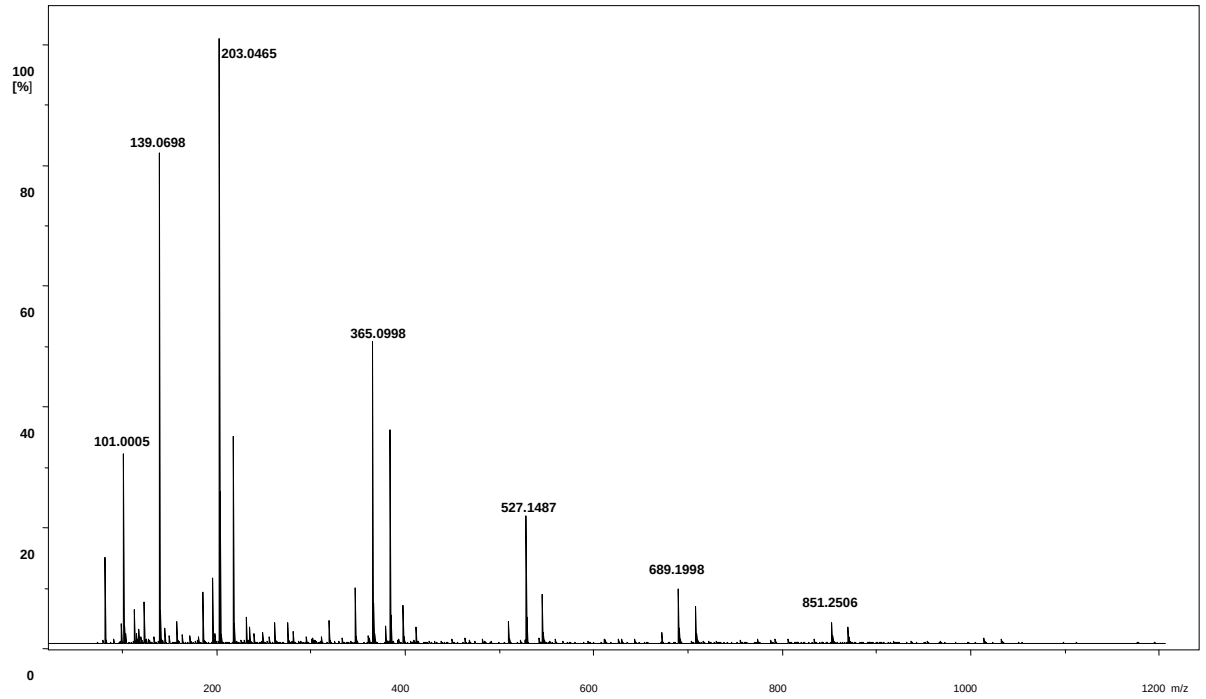

b)

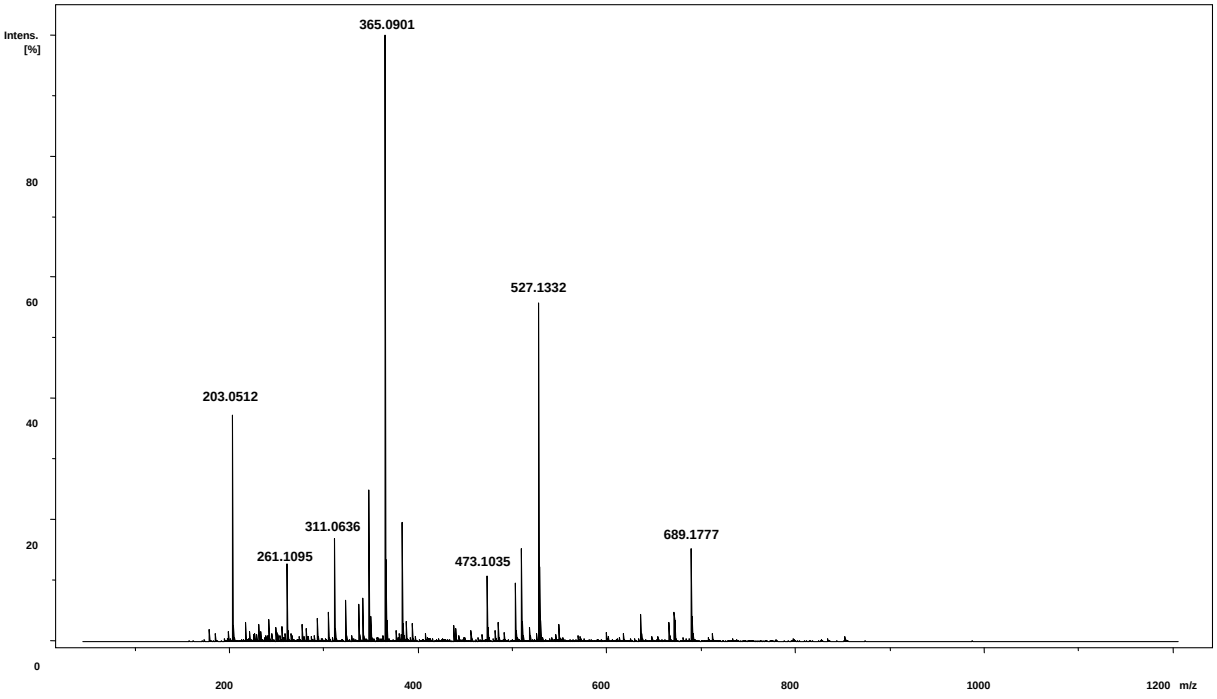

c)

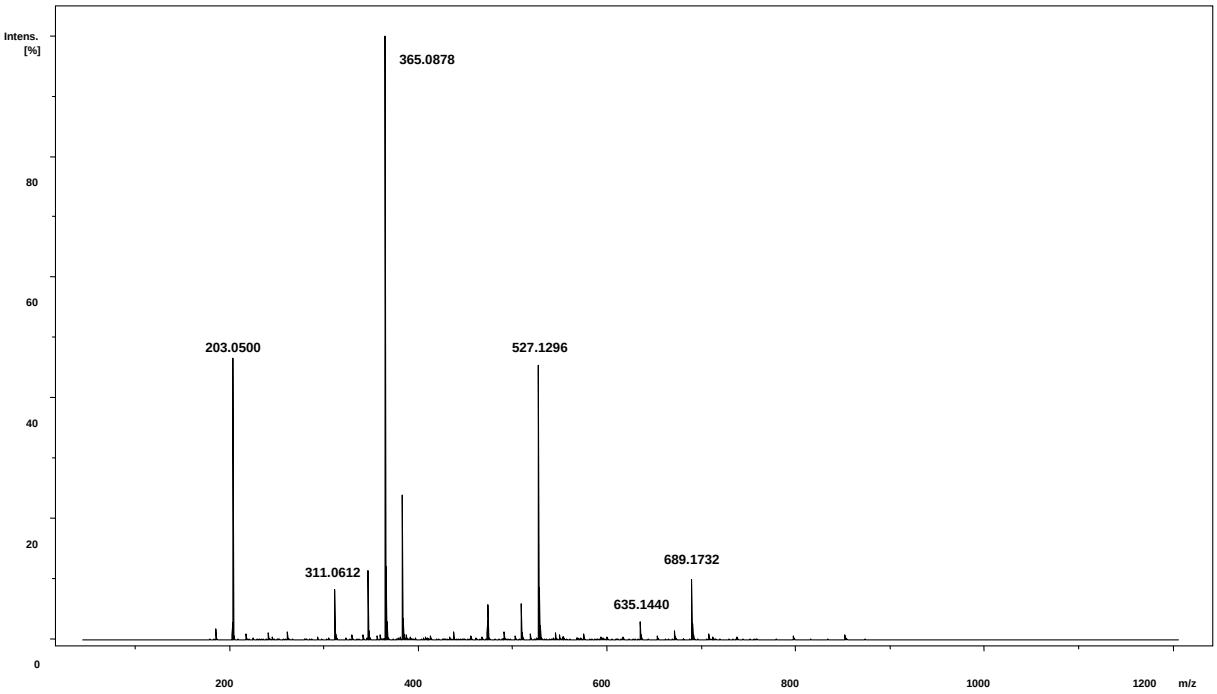

Figure S1. Mass spectra of caramelised: a) fructose, b) galactose and c) mannose in the positive ion mode using a direct infusion into an ESI-TOF-MS instrument

Table S1 High resolution mass (MS-TOF) data of caramelised: a) fructose, b) galactose, c) ribose, d) arabinose and their parent ions (M-H) in the negative ion mode

a)

Peak numbering	Assignment	Mol. Formula	Experimental *m/z* [M-H]	Theoretical *m/z* [M-H]	Relative Error [ppm]
1		$C_9H_{18}O_2$	157.1236	157.1234	1.5
2	Fru - H_2O	$C_6H_{10}O_5$	161.0457	161.0455	0.7
3	Fru	$C_6H_{12}O_6$	179.0561	179.0561	0.0
4		$C_7H_{14}O_8$	225.0608	225.0616	3.7
5		$C_{14}H_{28}O_2$	227.2018	227.2017	0.7
6		$C_{15}H_{30}O_2$	241.2181	241.2173	3.3
7		$C_{16}H_{32}O_2$	255.2341	255.2330	4.6
8		$C_{18}H_{36}O_2$	283.2653	283.2643	3.8
9		$C_{12}H_{16}O_8$	287.0765	287.0772	2.8
10		$C_{17}H_{26}O_4$	293.1760	293.1758	0.7
11	$(Fru)_2$ - $2\times H_2O$	$C_{12}H_{18}O_9$	305.0891	305.0878	4.3
12	$(Fru)_2$ - H_2O	$C_{12}H_{20}O_{10}$	323.0977	323.0984	2.0
13	$(Fru)_2$	$C_{12}H_{22}O_{11}$	341.1083	341.1089	1.9
14	$(Fru)_2$ + H_2O	$C_{12}H_{24}O_{12}$	359.1189	359.1195	1.7
15		$C_{13}H_{24}O_{13}$	387.1150	387.1144	1.5
16		$C_{22}H_{44}O_8$	435.2970	435.2963	1.5
17	$(Fru)_3$ - $3\times H_2O$	$C_{18}H_{26}O_{13}$	449.1305	449.1301	0.9
18	$(Fru)_3$ - $2\times H_2O$	$C_{18}H_{28}O_{14}$	467.1408	467.1406	0.4
19	$(Fru)_3$ - H_2O	$C_{18}H_{30}O_{15}$	485.1518	485.1512	1.3

20	$(Fru)_3$	$C_{18}H_{32}O_{16}$	503.1628	503.1618	2.0
21	$(Fru)_3 + H_2O$	$C_{18}H_{34}O_{17}$	521.1710	521.1723	2.5
22	$(Fru)_4 - 3\times H_2O$	$C_{24}H_{36}O_{18}$	611.1846	611.1829	2.9
23	$(Fru)_4 - 2\times H_2O$	$C_{24}H_{38}O_{19}$	629.1920	629.1935	1.4
24	$(Fru)_4 - H_2O$	$C_{24}H_{40}O_{20}$	647.2027	647.2040	2.0
25	$(Fru)_4$	$C_{24}H_{42}O_{21}$	665.2134	665.2146	1.8
26	$(Fru)_4 + H_2O$	$C_{24}H_{44}O_{22}$	683.2268	683.2251	2.4
27	$(Fru)_5 - 3\times H_2O$	$C_{30}H_{46}O_{23}$	773.2334	773.2357	2.9
28	$(Fru)_5 - 2\times H_2O$	$C_{30}H_{48}O_{24}$	791.2431	791.2463	4.0
29	$(Fru)_5 - H_2O$	$C_{30}H_{50}O_{25}$	809.2545	809.2568	2.9
30	$(Fru)_5$	$C_{30}H_{52}O_{26}$	827.2701	827.2674	3.2
31	$(Fru)_5 + H_2O$	$C_{30}H_{54}O_{27}$	845.2815	845.2780	4.2
32	$(Fru)_6 - H_2O$	$C_{36}H_{60}O_{30}$	971.3119	971.3097	2.3
33	$(Fru)_6$	$C_{36}H_{62}O_{31}$	989.3173	989.3202	2.9

b)

Peak numbering	Assignment	Mol. Formula	Experimental *m/z* [M-H]	Theoretical *m/z* [M-H]	Relative Error [ppm]
1		$C_6H_{12}O_2$	115.0767	115.0765	2.1
2		$C_7H_6O_2$	121.0294	121.0295	0.7
3		$C_4H_8O_4$	119.0349	119.0350	0.7
4		$C_7H_{14}O_2$	129.0925	129.0921	3.0
5		$C_8H_{16}O_2$	143.1084	143.1078	4.9
6		$C_9H_{18}O_2$	157.1236	157.1234	1.0
7	Gal - H_2O	$C_6H_{10}O_5$	161.0461	161.0455	3.7
8	Galactose	$C_6H_{12}O_6$	179.0564	179.0561	1.4
9		$C_7H_{14}O_8$	225.0608	225.0616	3.6
10		$C_{16}H_{32}O_2$	255.2324	255.2330	2.0
11		$C_{15}H_{22}O_4$	265.1452	265.1445	2.5
12		$C_9H_{18}O_9$	269.0869	269.0878	3.5
13		$C_{18}H_{36}O_2$	283.2629	283.2643	4.6
14	$(Gal)_2$ - 3×H_2O	$C_{12}H_{16}O_8$	287.0769	287.0772	1.2
15		$C_{17}H_{26}O_4$	293.1758	293.1758	0.1
16	$(Gal)_2$ - 2×H_2O	$C_{12}H_{18}O_9$	305.0863	305.0878	4.9
17	$(Gal)_2$ - H_2O	$C_{12}H_{20}O_{10}$	323.0985	323.0984	0.3
18	$(Gal)_2$	$C_{12}H_{22}O_{11}$	341.1094	341.1089	1.3
19	$(Gal)_2$ + H_2O	$C_{12}H_{24}O_{12}$	359.1183	359.1195	3.2
20	$(Gal)_3$ - 4×H_2O	$C_{18}H_{24}O_{12}$	431.1211	431.1195	3.8
21	$(Gal)_3$- 3×H_2O	$C_{18}H_{26}O_{13}$	449.1281	449.1301	4.4
22	$(Gal)_3$- 2×H_2O	$C_{18}H_{28}O_{14}$	467.1401	467.1406	1.2

23	$(Gal)_3 - H_2O$	$C_{18}H_{30}O_{15}$	485.1500	485.1512	2.4
24	$(Gal)_3$	$C_{18}H_{32}O_{16}$	503.1606	503.1618	2.3
25	$(Gal)_3 + H_2O$	$C_{18}H_{34}O_{17}$	521.1729	521.1723	1.1
26	$(Gal)_4 - 3\times H_2O$	$C_{24}H_{36}O_{18}$	611.1805	611.1829	3.9
27	$(Gal)_4 - 2\times H_2O$	$C_{24}H_{38}O_{19}$	629.1907	629.1935	4.4
28	$(Gal)_4 - H_2O$	$C_{24}H_{40}O_{20}$	647.2021	647.2040	3.0
29	$(Gal)_4$	$C_{24}H_{42}O_{21}$	665.2135	665.2146	1.6
30	$(Gal)_4 + H_2O$	$C_{24}H_{44}O_{22}$	683.2222	683.2251	4.3
31	$(Gal)_5 - 5\times H_2O$	$C_{30}H_{42}O_{21}$	737.2156	737.2146	1.4
32	$(Gal)_5 - 4\times H_2O$	$C_{30}H_{44}O_{22}$	755.2227	755.2251	3.2
33	$(Gal)_5 - 3\times H_2O$	$C_{30}H_{46}O_{23}$	773.2324	773.2357	4.2
34	$(Gal)_5 - 2\times H_2O$	$C_{30}H_{48}O_{24}$	791.2425	791.2463	4.7
35	$(Gal)_5 - H_2O$	$C_{30}H_{50}O_{25}$	809.2538	809.2568	3.4
36	$(Gal)_5$	$C_{30}H_{52}O_{26}$	827.2671	827.2674	0.3
37	$(Gal)_5 + H_2O$	$C_{30}H_{54}O_{27}$	845.2752	845.2780	3.0
38	$(Gal)_6 - 3\times H_2O$	$C_{36}H_{56}O_{28}$	935.2877	935.2885	0.9
39	$(Gal)_6 - 2\times H_2O$	$C_{36}H_{58}O_{29}$	953.3013	953.2991	2.3
40	$(Gal)_6 - H_2O$	$C_{36}H_{60}O_{30}$	971.3096	971.3097	0.0
41	$(Gal)_6$	$C_{36}H_{62}O_{31}$	989.3187	989.3202	1.5
42	$(Gal)_6 + H_2O$	$C_{36}H_{64}O_{32}$	1007.3352	1007.3308	4.3

c)

Peak numbering	Assignment	Mol. Formula	Theoretical *m/z* $[M-H]^-$	Experimental *m/z* $[M-H]^-$	Relative Error [ppm]
1	Rib - $2\times H_2O$	$C_5H_6O_3$	113.0244	113.0246	1.7
2	Rib - H_2O	$C_5H_8O_4$	131.0350	131.0344	4.4
3	Ribose	$C_5H_{10}O_5$	149.0455	149.0456	0.5
4	Rib + HCOOH	$C_6H_{12}O_7$	195.0510	195.0516	3.0
6	$(Rib)_2$ - $3\times H_2O$	$C_{10}H_{12}O_6$	227.0561	227.0572	4.7
7	$(Rib)_2$ - $2\times H_2O$	$C_{10}H_{14}O_7$	245.0667	245.0666	0.5
8	$(Rib)_2$ - H_2O	$C_{10}H_{16}O_8$	263.0772	267.0779	2.4
9	$(Rib)_2$	$C_{10}H_{18}O_9$	281.0878	281.0864	5.0
10		$C_{11}H_{16}O_9$	291.0722	291.0714	2.4
11	$(Rib)_2$ + HCOOH	$C_{11}H_{20}O_{11}$	327.0933	327.0923	2.9
12	$(Rib)_3$ - $3\times H_2O$	$C_{15}H_{20}O_{10}$	359.0984	359.0994	3.0
13	$(Rib)_3$ - $2\times H_2O$	$C_{15}H_{22}O_{11}$	377.1089	377.1090	0.1
14	$(Rib)_3$ - H_2O	$C_{15}H_{24}O_{12}$	395.1195	395.1199	1.0
15	$(Rib)_3$	$C_{15}H_{26}O_{13}$	413.1301	413.1293	1.8
16	$(Rib)_3$ + HCOOH	$C_{16}H_{28}O_{15}$	459.1355	459.1355	0.1
17	$(Rib)_4$ - $3\times H_2O$	$C_{20}H_{28}O_{14}$	491.1406	491.1378	2.8
18	$(Ryb)_4$ - $2\times H_2O$	$C_{20}H_{30}O_{15}$	509.1512	509.1487	4.9
19	$(Ryb)_4$ - H_2O	$C_{20}H_{32}O_{16}$	527.1618	527.1609	1.7
20	$(Ryb)_4$	$C_{20}H_{34}O_{17}$	545.1723	545.1739	2.8
21	$(Ryb)_4$ + H_2O	$C_{20}H_{36}O_{18}$	563.1829	563.1829	0.0
22	$(Ryb)_4$ + HCOOH	$C_{21}H_{36}O_{19}$	591.1778	591.1793	2.5
23	$(Rib)_5$ - $3\times H_2O$	$C_{25}H_{36}O_{18}$	623.1829	623.1751	7.8

24	$(Rib)_5$ - 2×H_2O	$C_{25}H_{38}O_{19}$	641.1935	641.1904	4.7
25	$(Rib)_5$ - H_2O	$C_{25}H_{40}O_{20}$	659.2040	659.2033	1.1
26	$(Rib)_5$	$C_{25}H_{42}O_{21}$	677.2146	677.2162	2.3
27	$(Rib)_5$ + H_2O	$C_{25}H_{44}O_{22}$	695.2251	695.2266	2.1
28	$(Rib)_5$ + HCOOH	$C_{26}H_{44}O_{23}$	723.2201	723.2236	4.9
30	$(Rib)_6$ - 3×H_2O	$C_{30}H_{44}O_{22}$	755.2252	755.2272	2.0
31	$(Rib)_6$ - 2×H_2O	$C_{30}H_{46}O_{23}$	773.2357	773.2327	3.1
32	$(Rib)_6$ - H_2O	$C_{30}H_{48}O_{24}$	791.2463	791.2450	1.6
33	$(Rib)_6$	$C_{30}H_{50}O_{25}$	809.2568	809.2604	4.4
34	$(Rib)_6$ + H_2O	$C_{30}H_{52}O_{26}$	827.2674	827.2709	4.2

d)

Peak numbering	**Assignment**	**Mol. Formula**	**Experimental *m/z* [M-H]$^-$**	**Theoretical *m/z* [M-H$^-$**	**Relative Error [ppm]**
1	Ara - H_2O	$C_5H_8O_4$	131.0350	131.0350	0.1
2	Arabinose	$C_5H_{10}O_5$	149.0454	149.0455	1.0
3	$(Ara)_2$ - 3×H_2O	$C_{10}H_{12}O_6$	227.0550	227.0561	5.0
4	$(Ara)_2$ - 2×H_2O	$C_{10}H_{14}O_7$	245.0673	245.0667	2.5
5	$(Ara)_2$ - H_2O	$C_{10}H_{16}O_8$	263.0761	263.0772	1.8
6	$(Ara)_2$	$C_{10}H_{18}O_9$	281.0867	281.0878	2.0
7	$(Ara)_2$ + H_2O	$C_{10}H_{20}O_{10}$	299.0972	299.0984	7.6

8	$(Ara)_2$ + HCOOH	$C_{11}H_{20}O_{11}$	327.0922	327.0933	2.3
9	$(Ara)_3$ - 2×H_2O	$C_{15}H_{22}O_{11}$	377.1078	377.1089	4.0
10	$(Ara)_3$ - H_2O	$C_{15}H_{24}O_{12}$	395.1184	395.1195	0.3
11	$(Ara)_3$	$C_{15}H_{26}O_{13}$	413.1290	413.1301	2.2
12	$(Ara)_3$ + H_2O	$C_{15}H_{28}O_{14}$	431.1395	431.1406	1.4
13	$(Ara)_3$ + HCOOH	$C_{16}H_{28}O_{15}$	459.1344	459.1355	2.8
14	$(Ara)_4$ - 2×H_2O	$C_{20}H_{30}O_{15}$	509.1501	509.1512	4.3
15	$(Ara)_4$ - H_2O	$C_{20}H_{32}O_{16}$	527.1607	527.1618	1.7
16	$(Ara)_4$	$C_{20}H_{34}O_{17}$	545.1712	545.1723	1.0
17	$(Ara)_4$ + H_2O	$C_{20}H_{36}O_{18}$	563.1818	563.1829	0.0
18	$(Ara)_4$ + HCOOH	$C_{21}H_{36}O_{19}$	591.1767	591.1778	0.4
19	$(Ara)_5$ - 2×H_2O	$C_{25}H_{38}O_{19}$	641.1924	641.1935	0.3
20	$(Ara)_5$ - H_2O	$C_{25}H_{40}O_{20}$	659.2029	659.2040	0.8
21	$(Ara)_5$	$C_{25}H_{42}O_{21}$	677.2135	677.2146	0.5
22	$(Ara)_5$ + H_2O	$C_{25}H_{44}O_{22}$	695.2241	695.2251	0.6
23	$(Ara)_5$ + HCOOH	$C_{26}H_{44}O_{23}$	723.2190	723.2201	1.9
24	$(Ara)_6$ - 2×H_2O	$C_{30}H_{46}O_{23}$	773.2346	773.2357	1.2
25	$(Ara)_6$ - H_2O	$C_{30}H_{48}O_{24}$	791.2452	791.2463	4.0
26	$(Ara)_6$	$C_{30}H_{50}O_{25}$	809.2557	809.2568	2.2
27	$(Ara)_6$ + H_2O	$C_{30}H_{52}O_{26}$	827.2663	827.2674	2.1
28	$(Ara)_6$ + HCOOH	$C_{31}H_{52}O_{27}$	855.2612	855.2623	0.9

a)

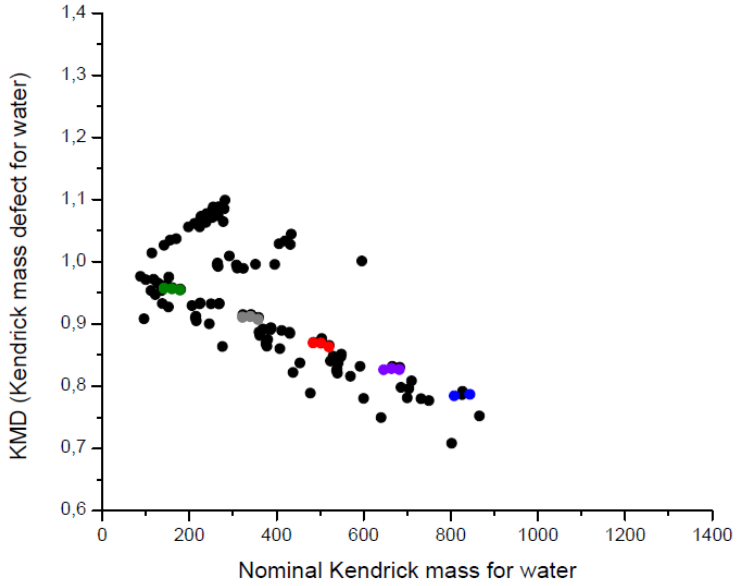

b)

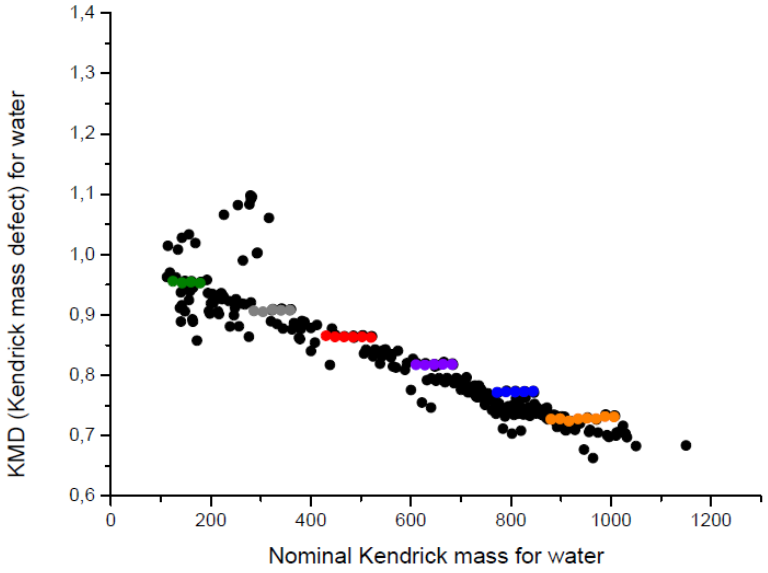

c)

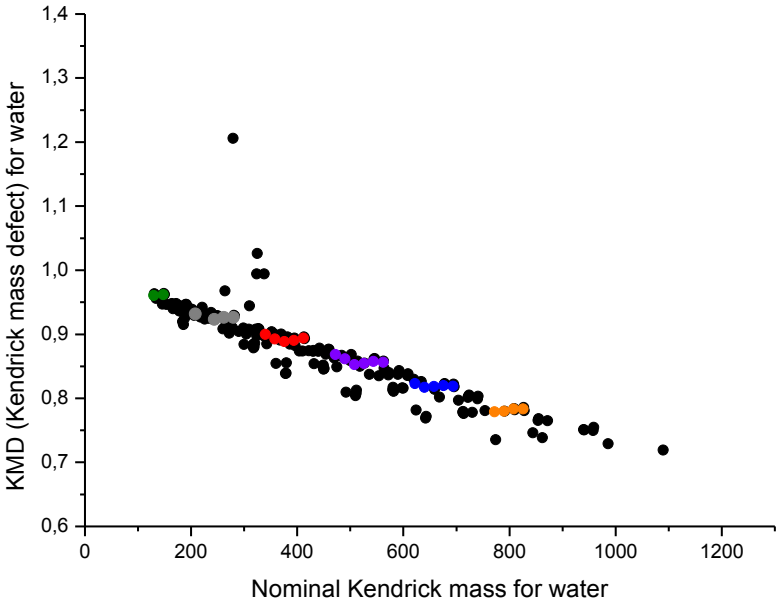

d)

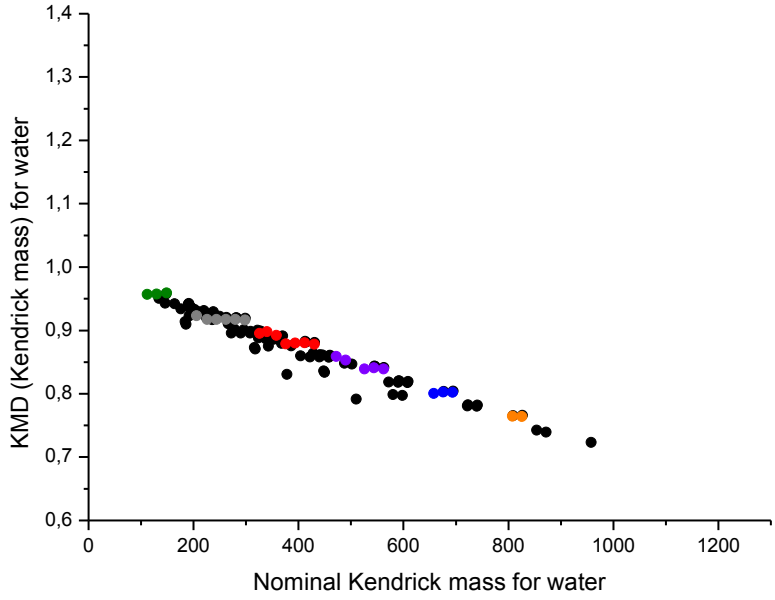

Figure S2 Two dimensional Kendrick plots for mass increment H_2O showing the distribution of the Kendrick mass defect plotted against the nominal Kendrick mass of pseudo-molecular ions for caramelised: a) fructose, b) galactose, c) ribose and d) arabinose in the negative ion mode. The colours indicate the homologous series of monomers, dimers, trimers, tetramers, pentamers, hexamers

a)

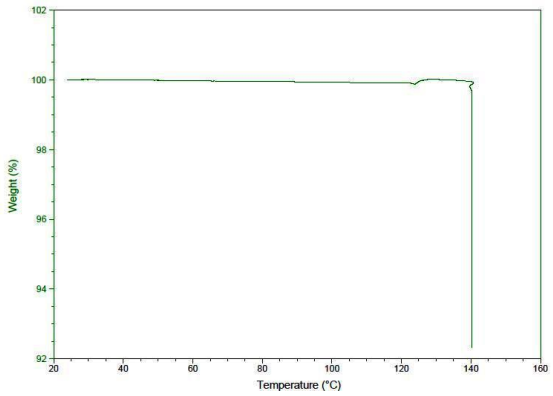

b)

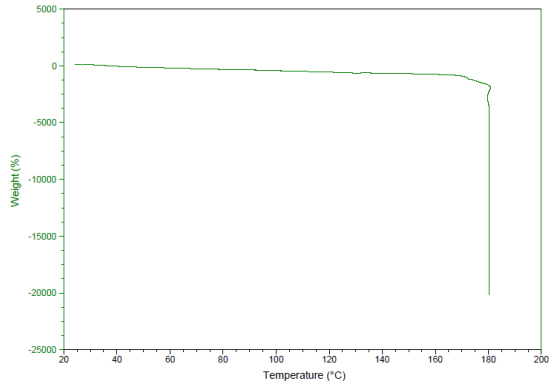

c)

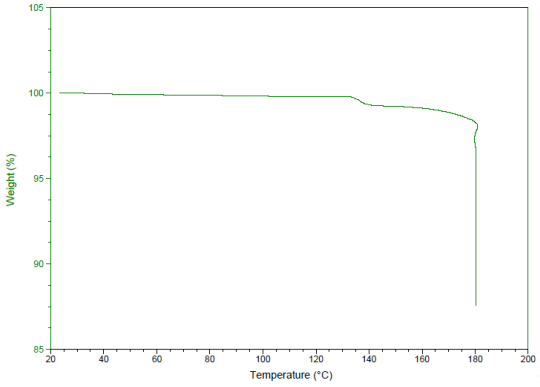

Figure S3 Thermogravimetric curves of caramelised: a) fructose, b) galactose and c) mannose. The temperature was ramped from 25 to 180 °C (140 °C, fructose) and kept at final temperature for 2 h

Figure S4 Infrared spectra of caramelized: a) fructose, b) galactose and c) mannose

a) IR: 3318.9, 2933.6, 2888.3, 1648.6, 1415.7, 1340.2, 1252.1, 1024.5, 978.9, 924.0, 866.4, 817.4, 778.6 cm^{-1}

b) IR: 3308.6, 2926.3, 2360.1, 2340.7, 1645.5, 1416.8, 1320.6, 1243.4, 1024.1, 773.7 cm^{-1}

c) IR: 3332.0, 2927.1, 2360.4, 1645.2, 1337.2, 995.8, 842.6, 783.14 cm^{-1}

a)

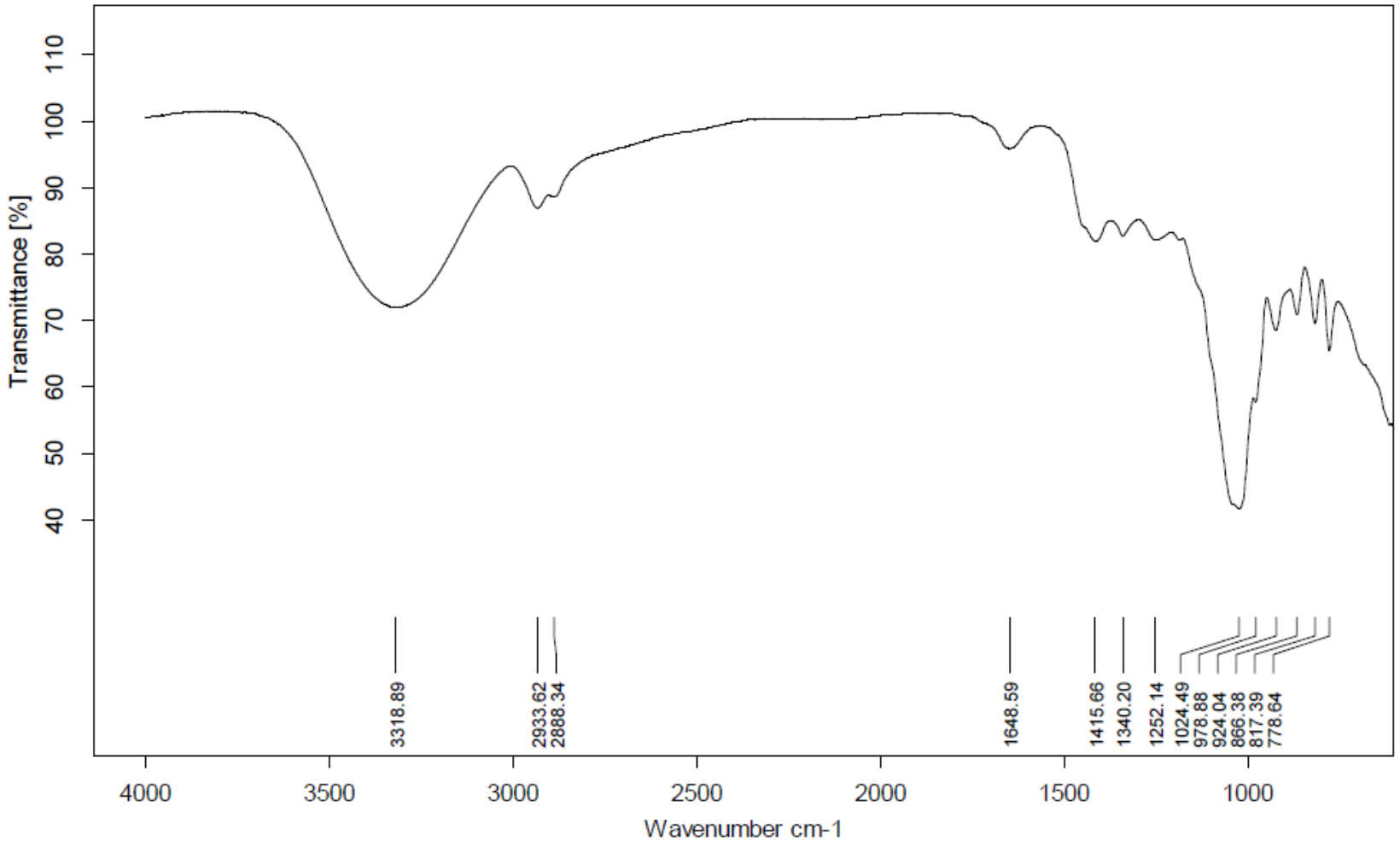

b)

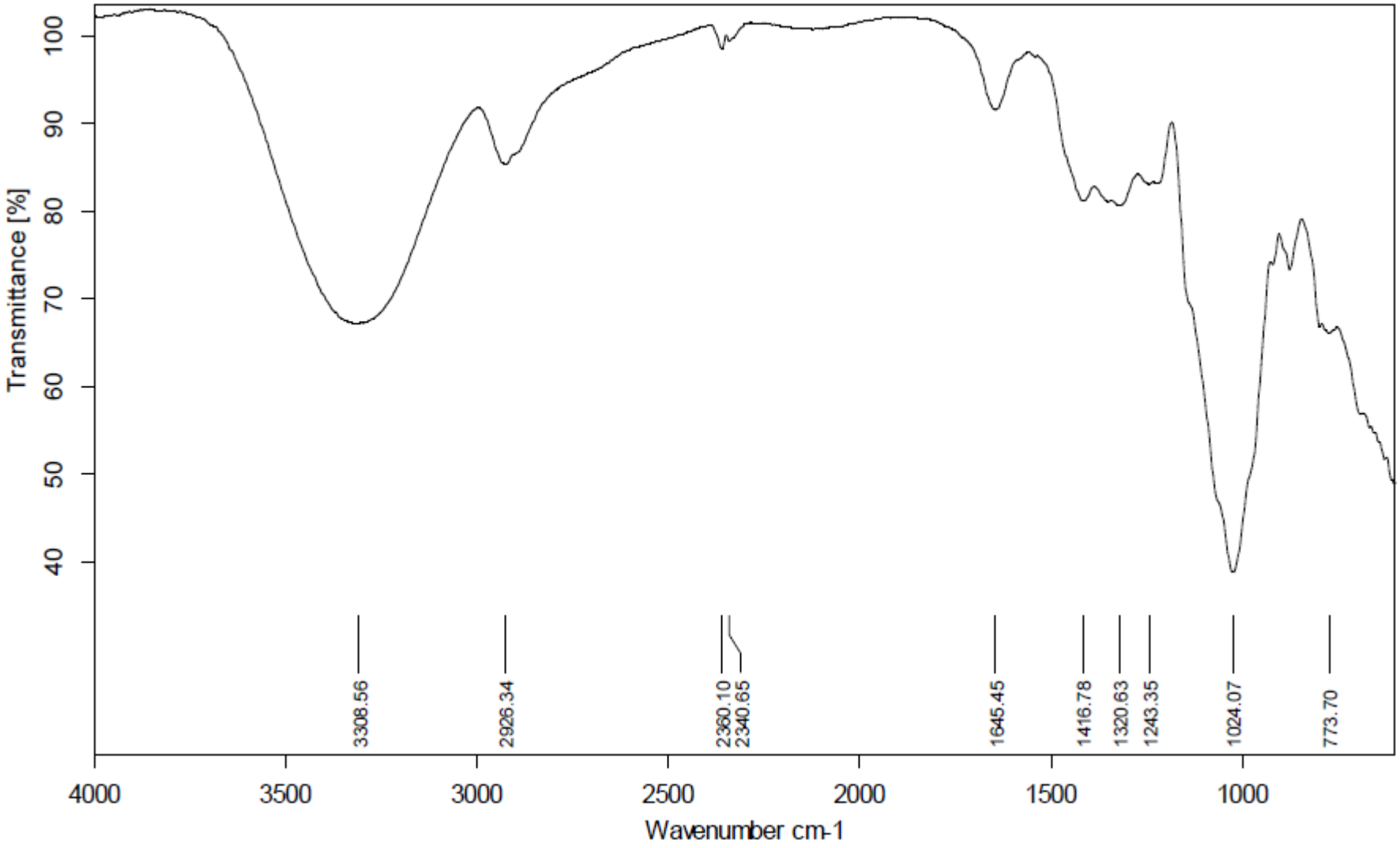

c)

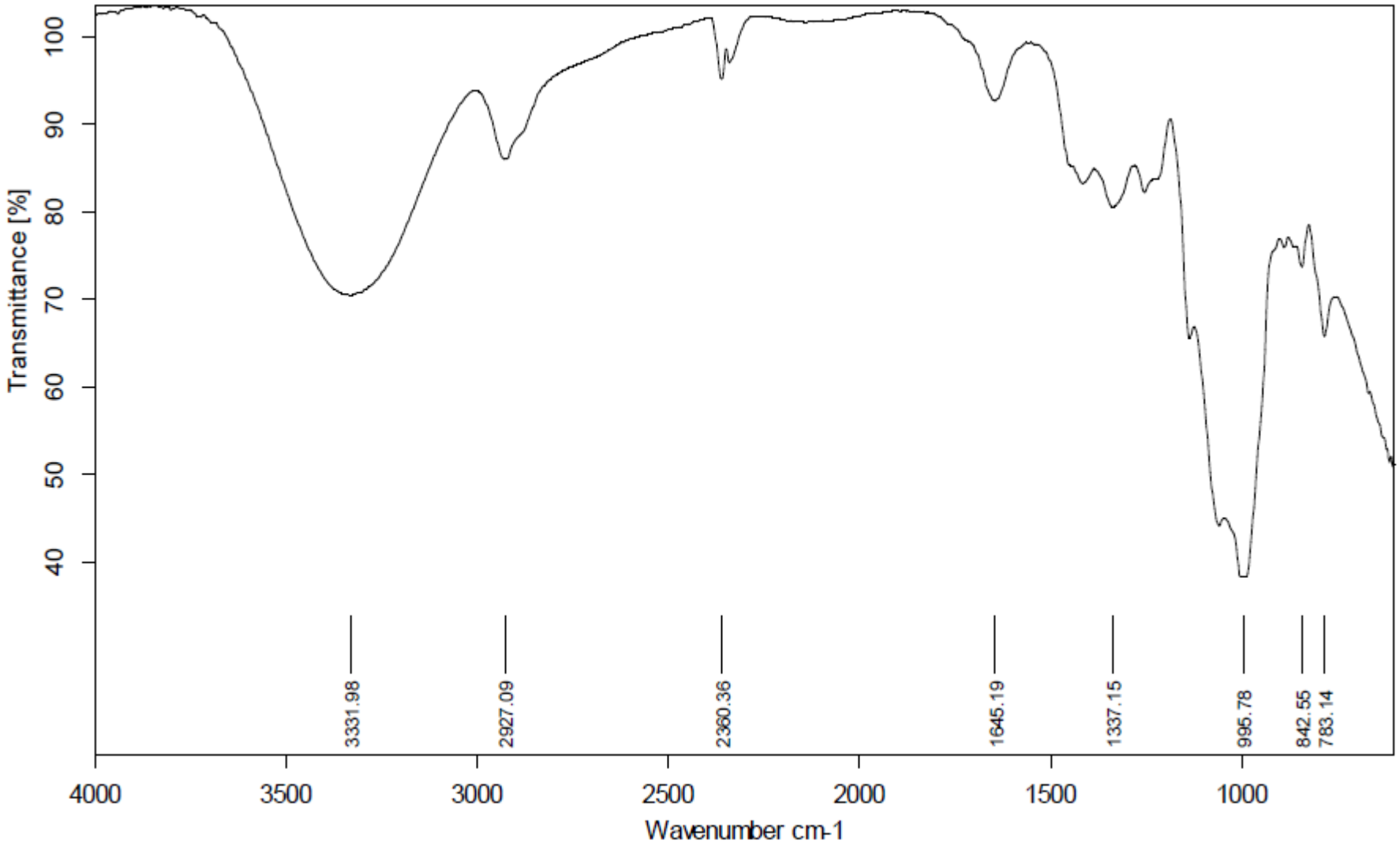

Figure S5 ^{1}H NMR spectra of caramelized: a) fructose, b) galactose and c) mannose

a) ^{1}H NMR (400 MHz, D_2O): δ 9.33 (CHO, m), 7.40 (m, Ar-H), 6.54 (m, Ar-H), 3.44-3.91 (m, >CHOH), 1.98 (m, -CH_3).

b) ^{1}H NMR (400 MHz, D_2O): δ 9.35 (CHO, m), 7.40 (m, Ar-H), 6.41 (m, Ar-H), 4.44-5.19 (m, >C=C-H), 3.35-4.13 (m, >CHOH).

c) ^{1}H NMR (400 MHz, D_2O): δ 9.31 (CHO, m), 7.39 (m, Ar-H), 6.52 (m, Ar-H), 4.92-5.25 (m, >C=C-H), 3.22-4.37 (m, >CHOH).

a) ^{1}H NMR

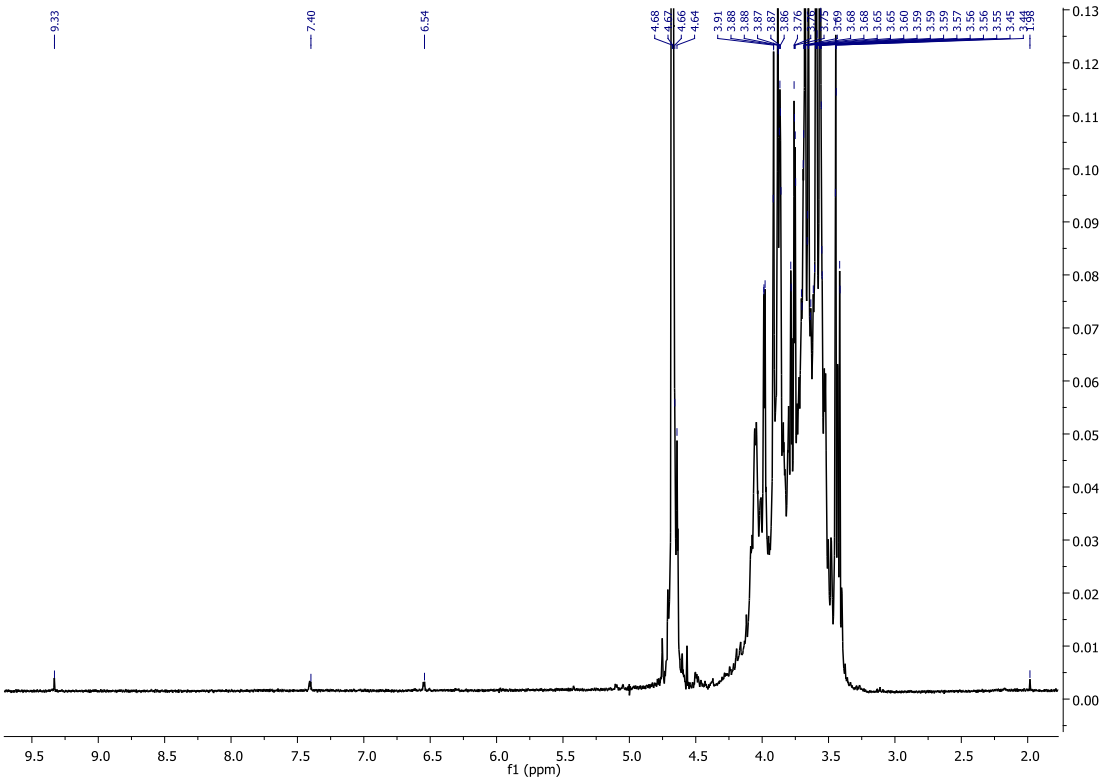

b) ^{1}H NMR

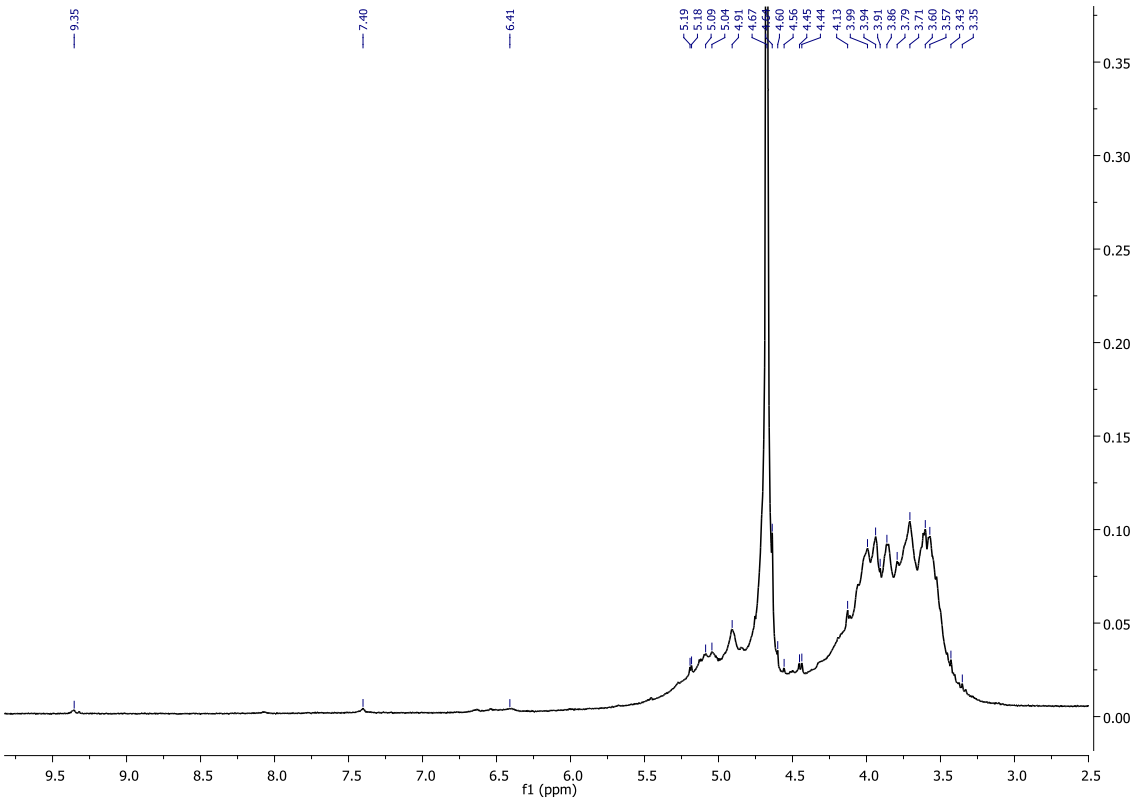
9.35
7.40
6.41
5.19
5.18
5.09
5.04
4.91
4.67
4.60
4.56
4.45
4.44
4.13
3.99
3.94
3.91
3.86
3.79
3.71
3.60
3.57
3.43
3.35
f1 (ppm)

c) ^{1}H NMR

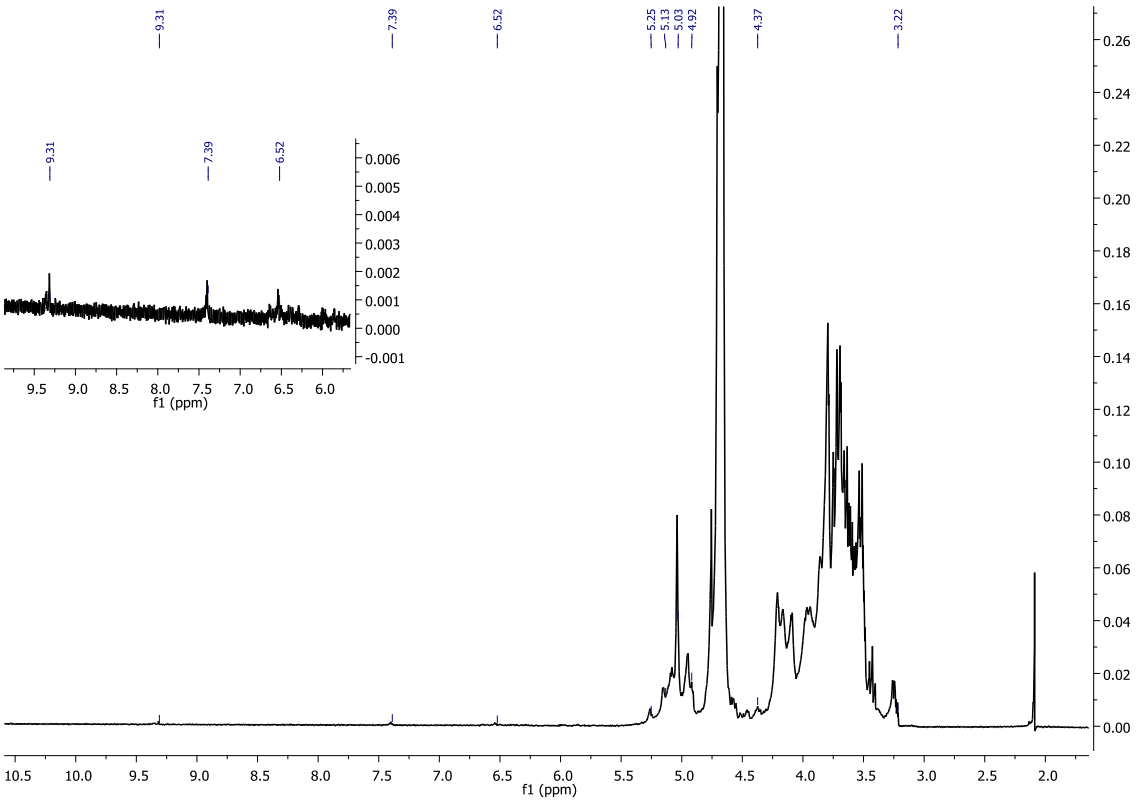
9.31
7.39
6.52
5.25
5.13
5.03
4.92
4.37
3.22
f1 (ppm)

Oligomers of hexose:

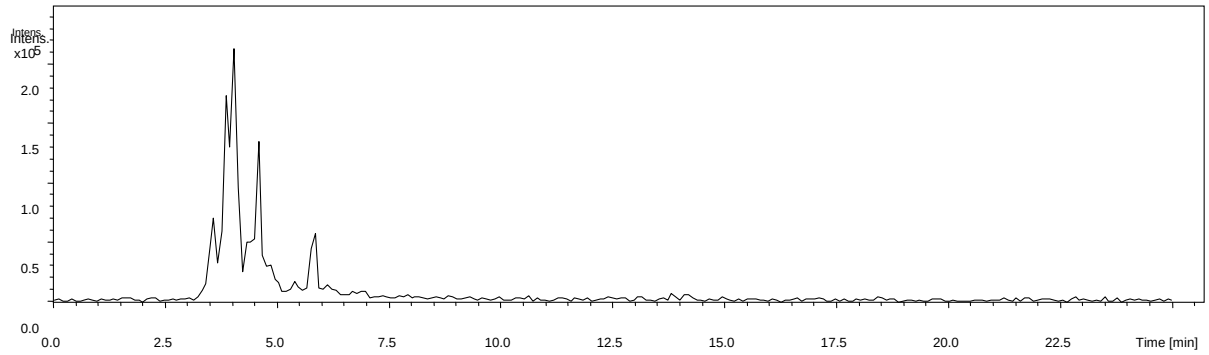

Figure S6 EIC at *m/z* 341.0 ($C_{12}H_{22}O_{11}$) for caramelised fructose in the negative ion mode

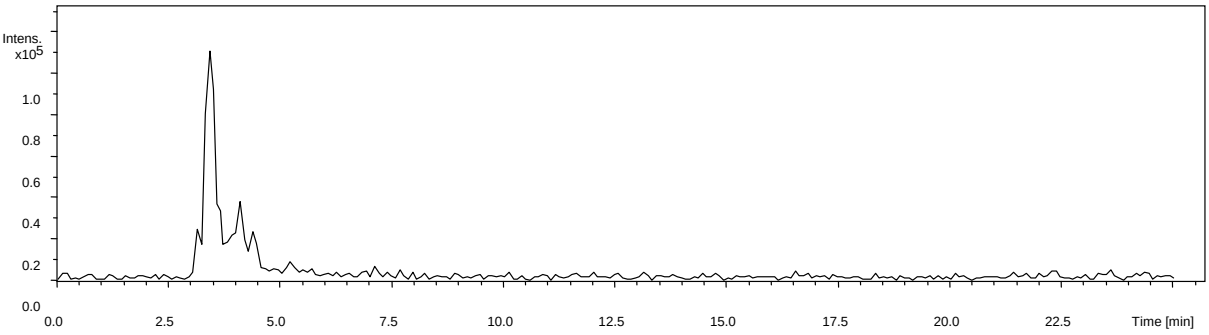

Figure S7 EIC at *m/z* 341.0 ($C_{12}H_{22}O_{11}$) for caramelised galactose in the negative ion mode

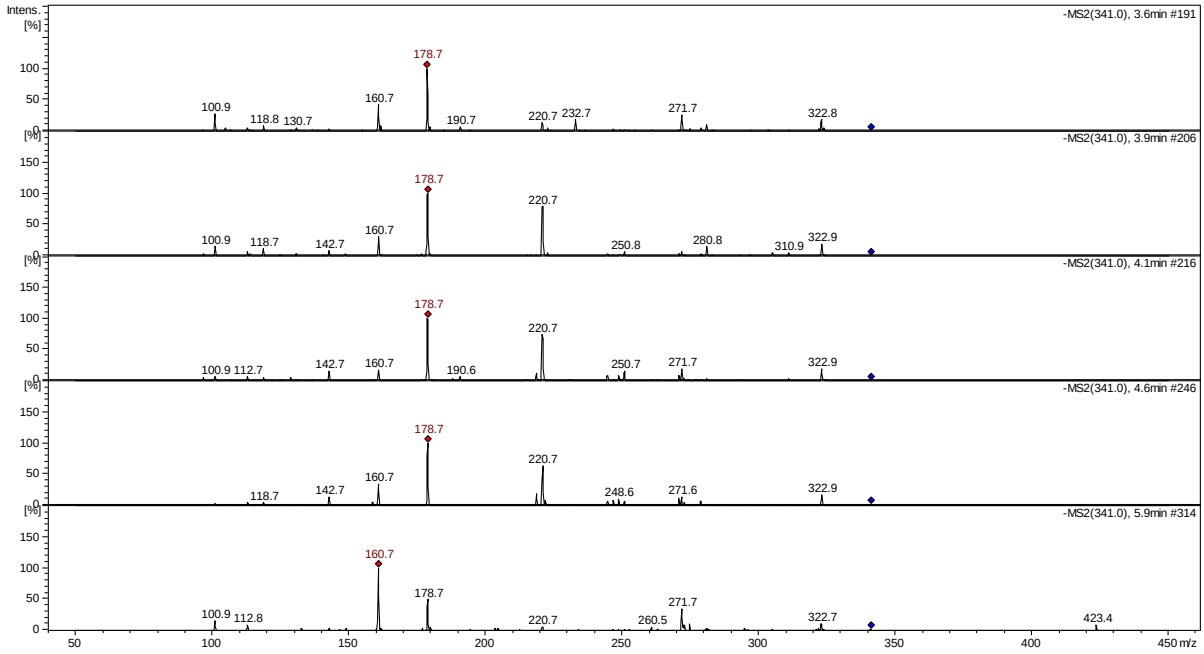

Figure S8 MS^2 spectra of fragment at *m/z* 341.0 ($C_{12}H_{22}O_{11}$) for five chromatographic peaks of caramelised fructose in the negative ion mode

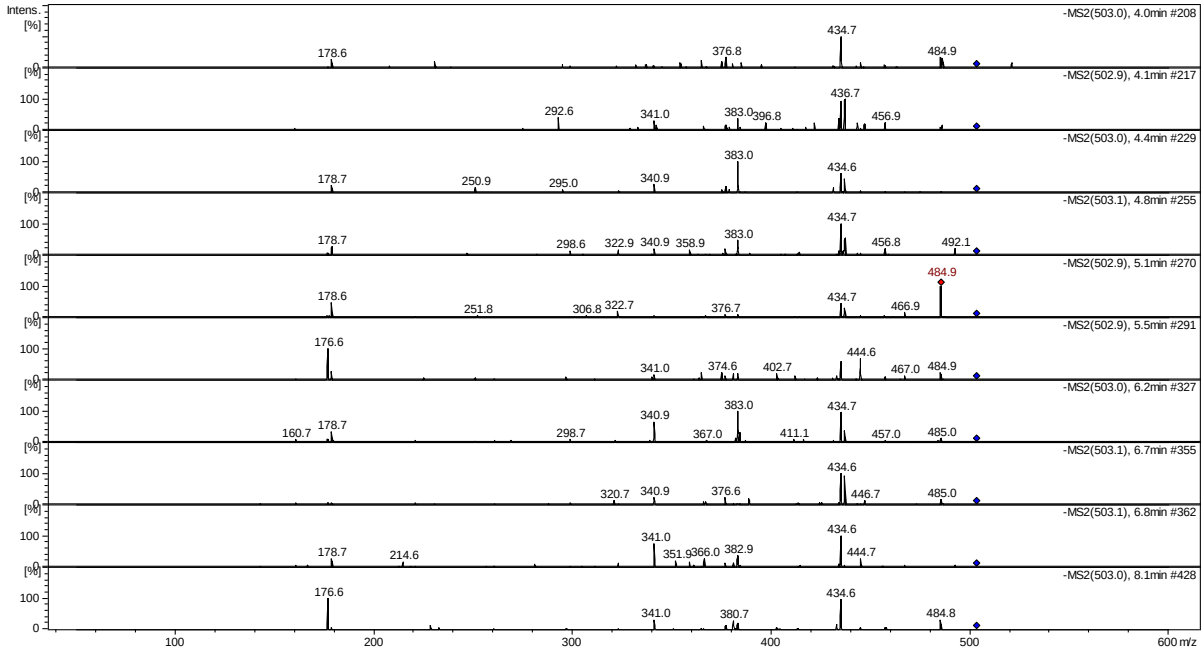

Figure S9 MS^2 spectra of fragment at *m/z* 503.0 ($C_{18}H_{32}O_{16}$) for ten chromatographic peaks of caramelised fructose in the negative ion mode

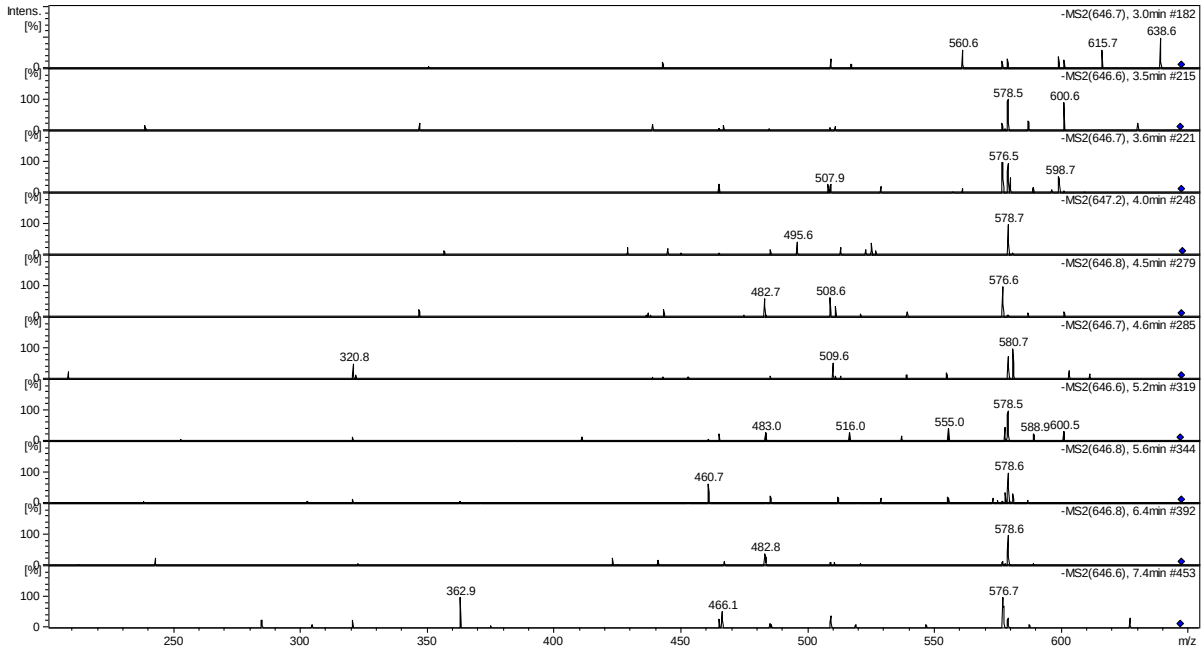

Figure S10 MS^2 spectra of fragment at *m/z* 647.0 ($C_{24}H_{40}O_{20}$) for ten chromatographic peaks of caramelised fructose in the negative ion mode

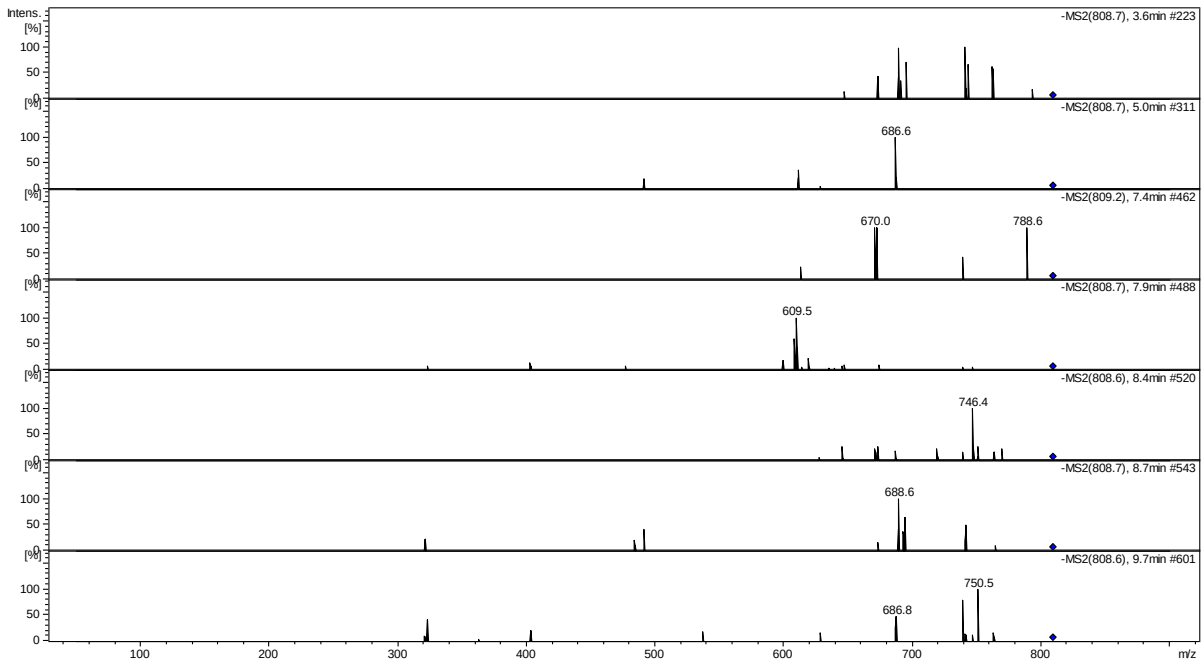

Figure S11 MS^2 spectra of fragment at *m/z* 809.0 ($C_{30}H_{50}O_{25}$) for seven chromatographic peaks of caramelised fructose in the negative ion mode

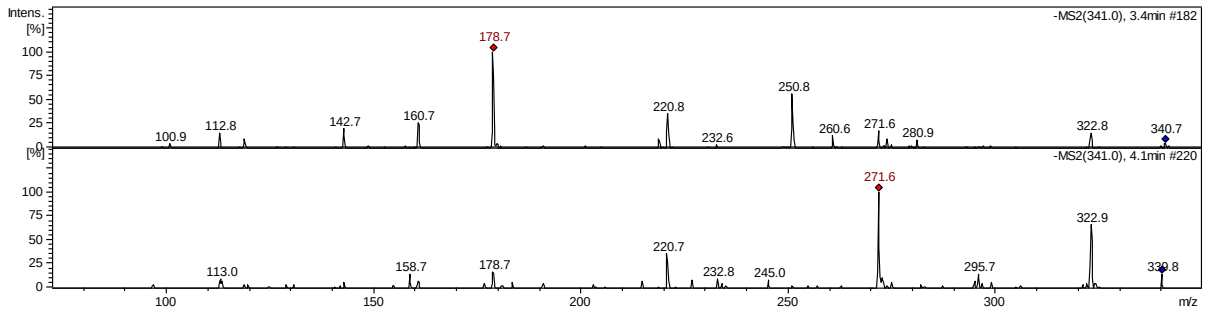

Figure S12 MS^2 spectra of fragment at *m/z* 341.0 ($C_{12}H_{22}O_{11}$) for two chromatographic peaks of caramelised galactose in the negative ion mode

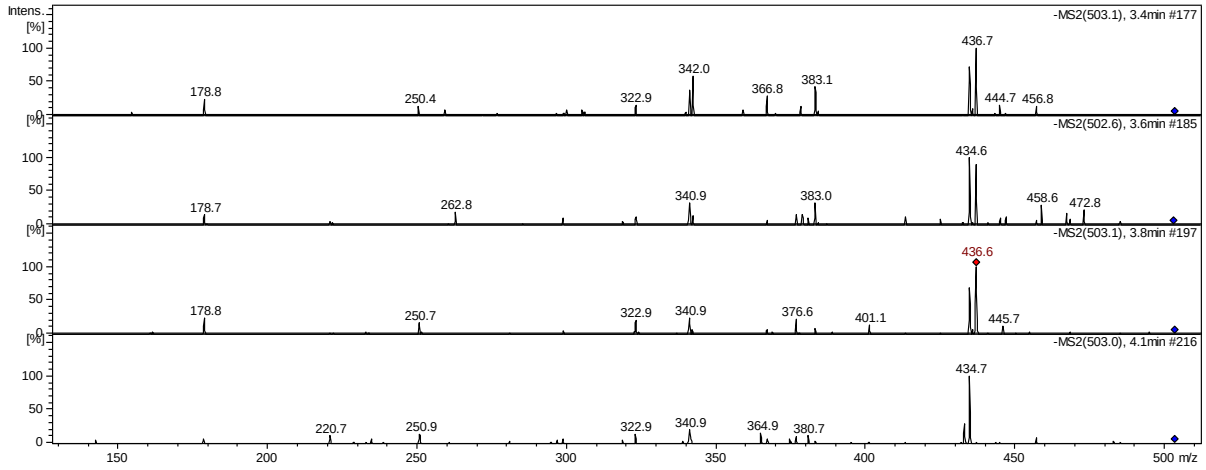

Figure S13 MS^2 spectra of fragment at *m/z* 503.0 ($C_{18}H_{32}O_{16}$) for four chromatographic peaks of caramelised galactose in the negative ion mode

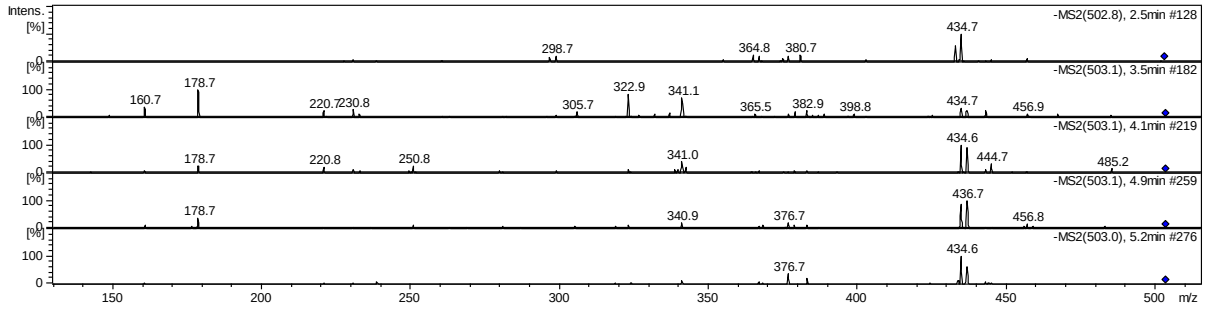

Figure S14 MS^2 spectra of fragment at *m/z* 503.0 ($C_{18}H_{32}O_{16}$) for four chromatographic peaks of caramelised mannose in the negative ion mode

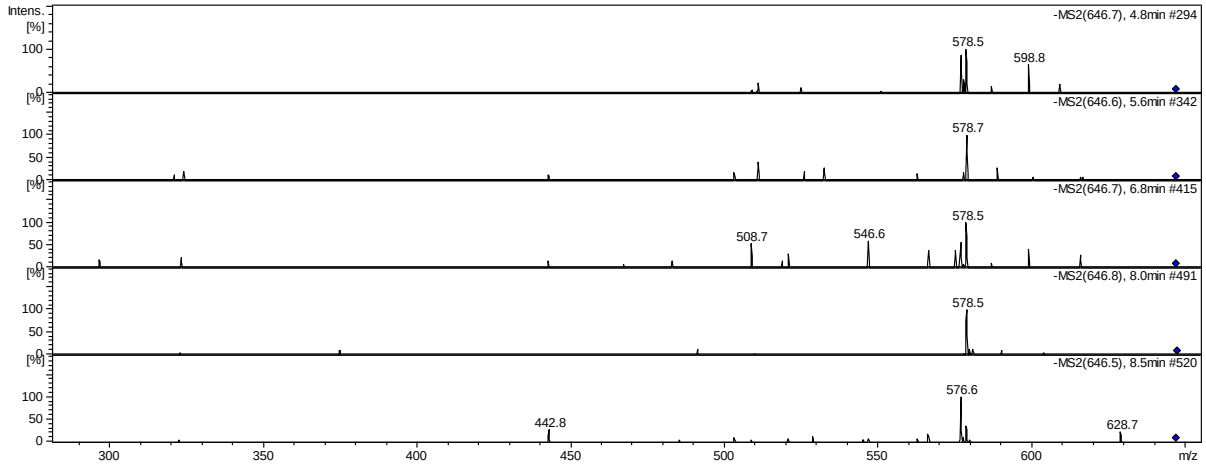

Figure S15 MS^2 spectra of fragment at *m/z* 647.0 ($C_{24}H_{40}O_{20}$) for ten chromatographic peaks of caramelised mannose in the negative ion mode

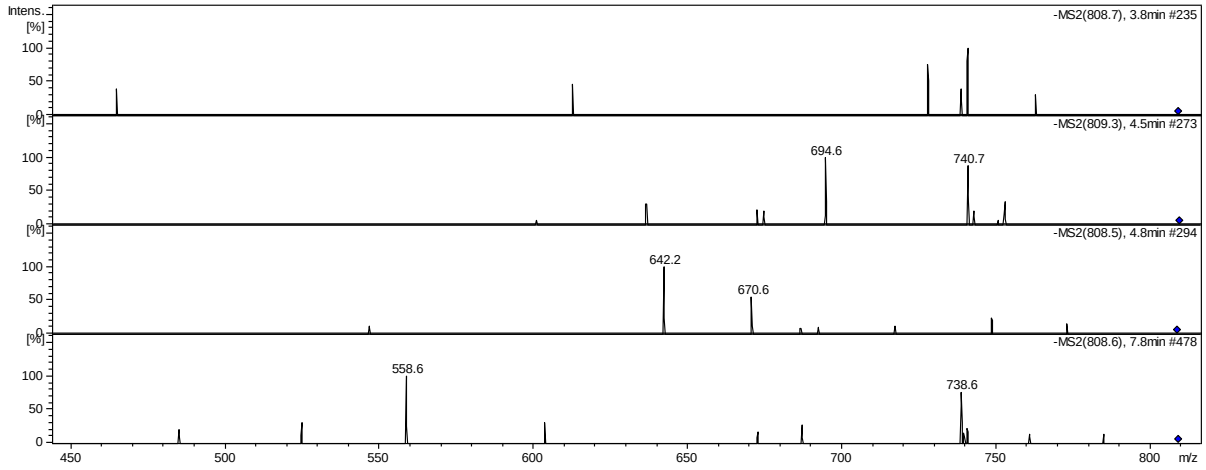

Figure S16 MS^2 spectra of fragment at *m/z* 809.0 ($C_{30}H_{50}O_{25}$) for seven chromatographic peaks of caramelised mannose in the negative ion mode

Dehydration products:

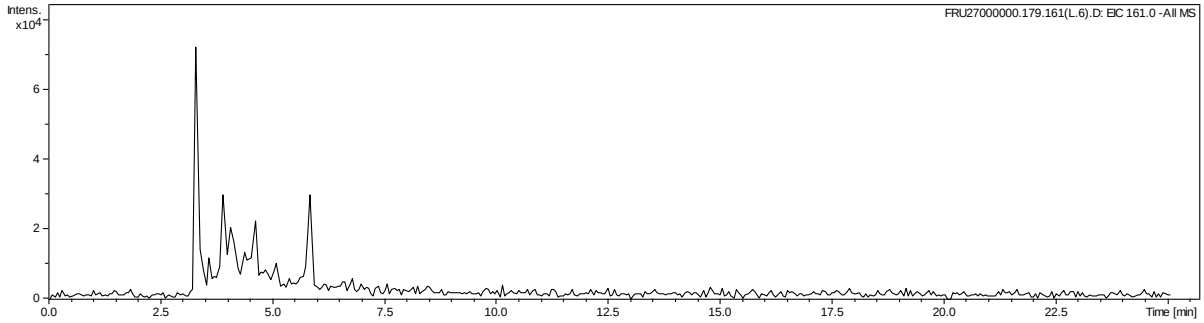

Figure S17 EIC at *m/z* 161.0 ($C_6H_{10}O_5$) for caramelised fructose in the negative ion mode

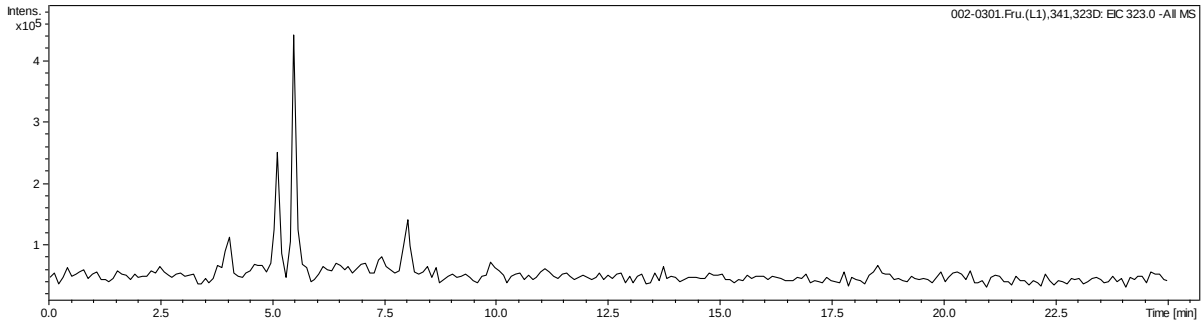

Figure S18 EIC at *m/z* 323.0 ($C_{12}H_{20}O_{10}$) for caramelised fructose in the negative ion mode

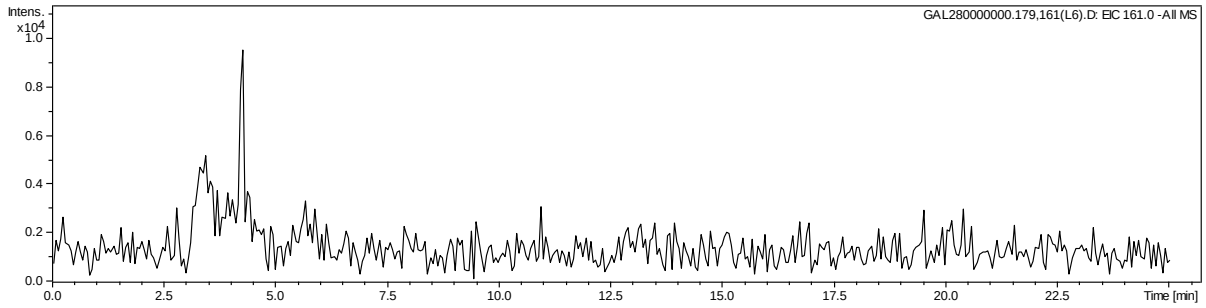

Figure S19 EIC at *m/z* 161.0 ($C_6H_{10}O_5$) for caramelised galactose in the negative ion mode

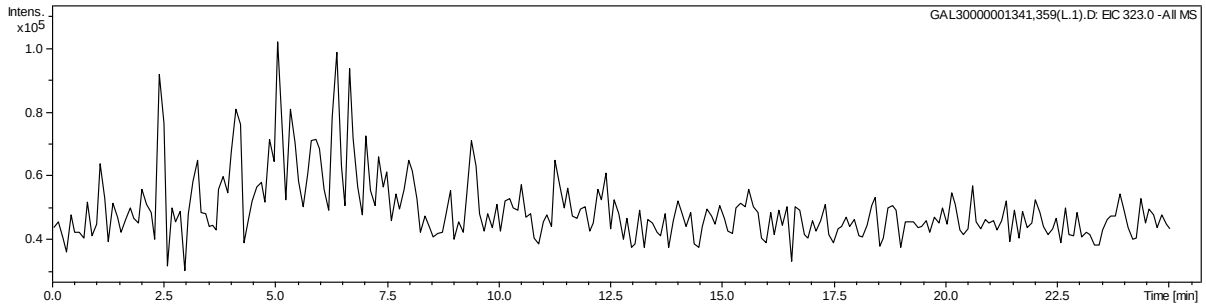

Figure S20 EIC at *m/z* 323.0 ($C_{12}H_{20}O_{10}$) for caramelised galactose in the negative ion mode

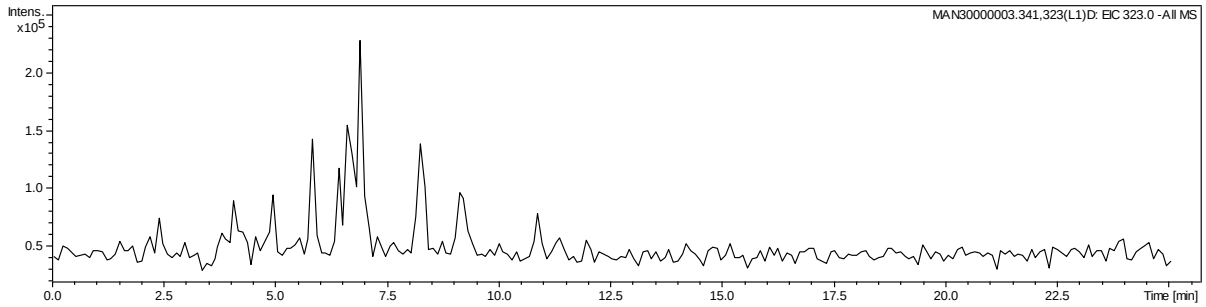

Figure S21 EIC at *m/z* 323.0 ($C_{12}H_{20}O_{10}$) for caramelised mannose in the negative ion mode

Hydration products:

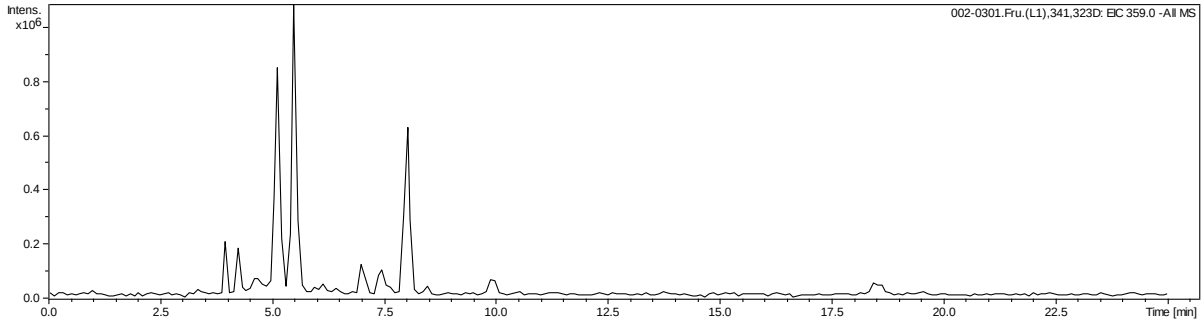

Figure S22 EIC at *m/z* 359.0 ($C_{12}H_{24}O_{12}$) for caramelised fructose in the negative ion mode

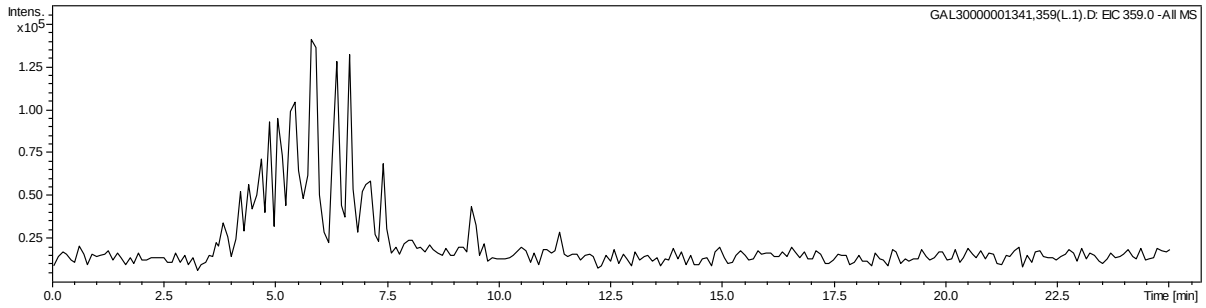

Figure S23 EIC at *m/z* 359.0 ($C_{12}H_{24}O_{12}$) for caramelised galactose in the negative ion mode

Monomer and oligomers of pentose:

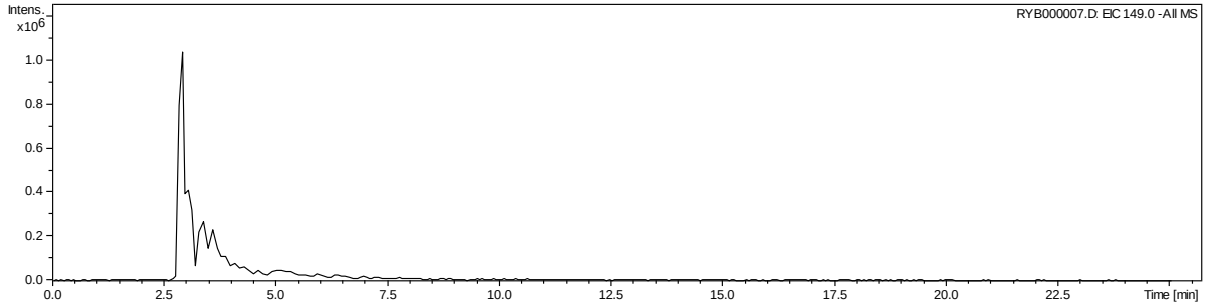

Figure S24 EIC at *m/z* 149.0 ($C_5H_{10}O_5$) for caramelised rybose in the negative ion mode

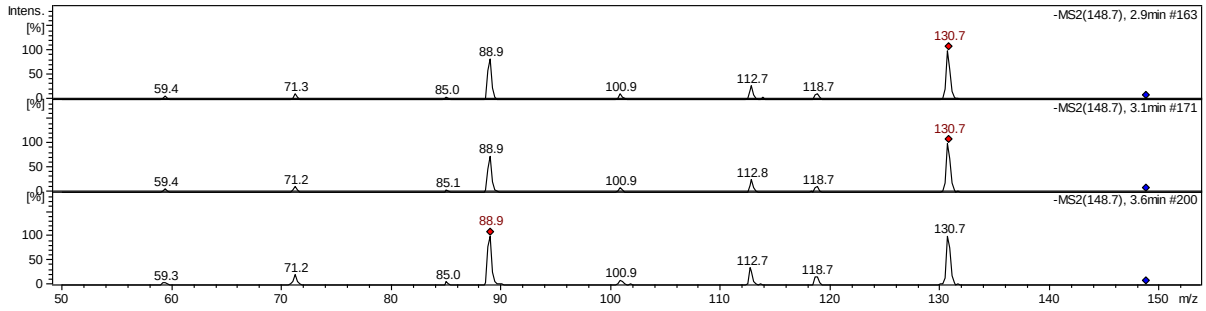

Figure S25 MS^2 spectra of fragment at *m/z* 149.0 ($C_5H_{10}O_5$) for three chromatographic peaks of caramelised rybose in the negative ion mode

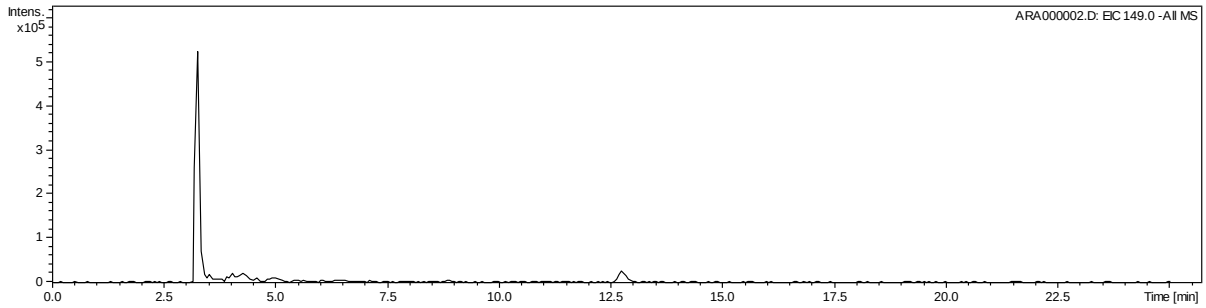

Figure S26 EIC at *m/z* 149.0 ($C_5H_{10}O_5$) for caramelised arabinose in the negative ion mode

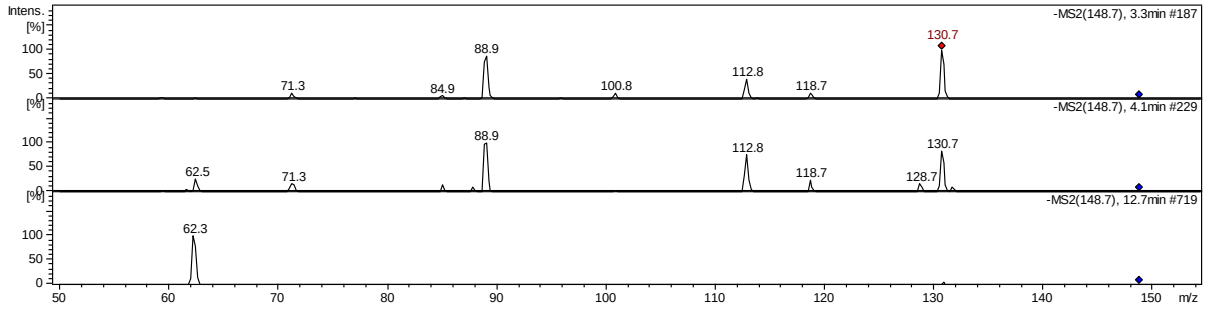

Figure S27 MS^2 spectra of fragment at *m/z* 149 ($C_5H_8O_4$) for three chromatographic peaks of caramelised arabinose in the negative ion mode

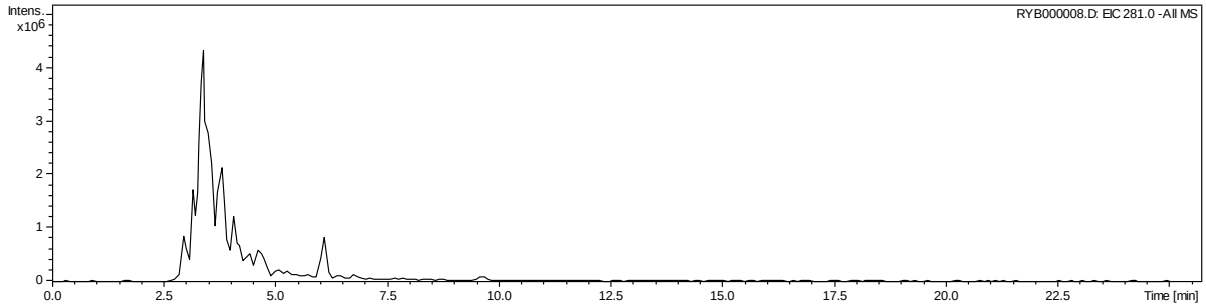

Figure S28 EIC at *m/z* 281.0 ($C_{10}H_{18}O_9$) for caramelised rybose in the negative ion mode

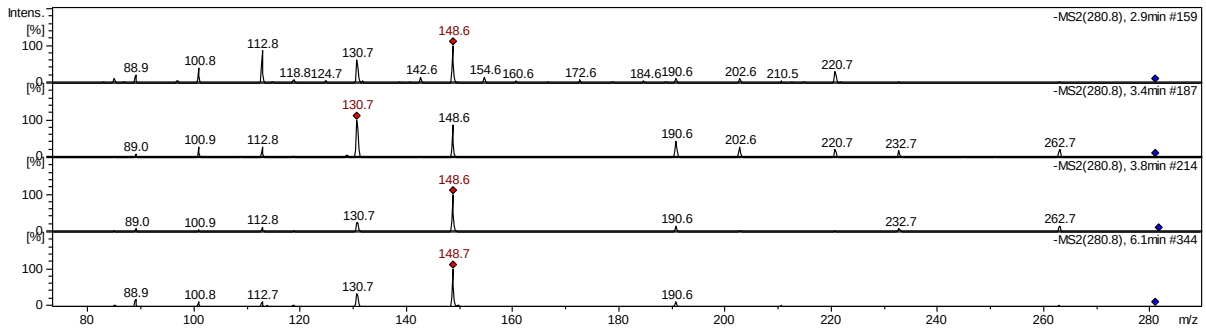

Figure S29 MS^2 spectra of fragment at *m/z* 281.0 ($C_{10}H_{18}O_9$) for four chromatographic peaks of caramelised rybose in the negative ion mode

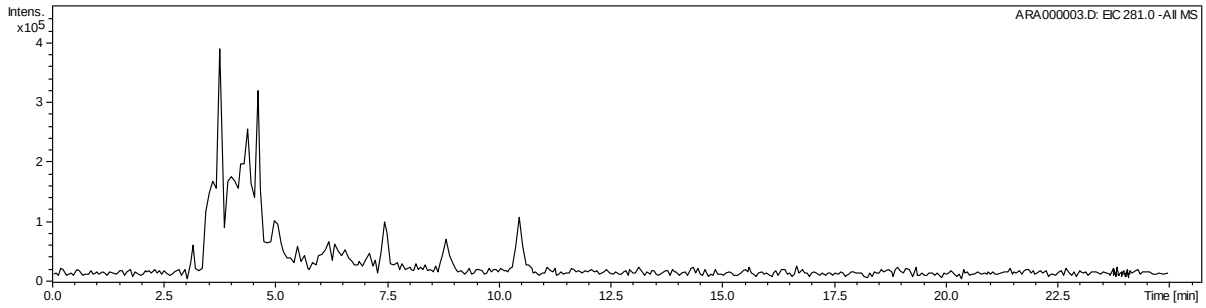

Figure S30 EIC at *m/z* 281.0 ($C_{10}H_{18}O_9$) for caramelised arabinose in the negative ion mode

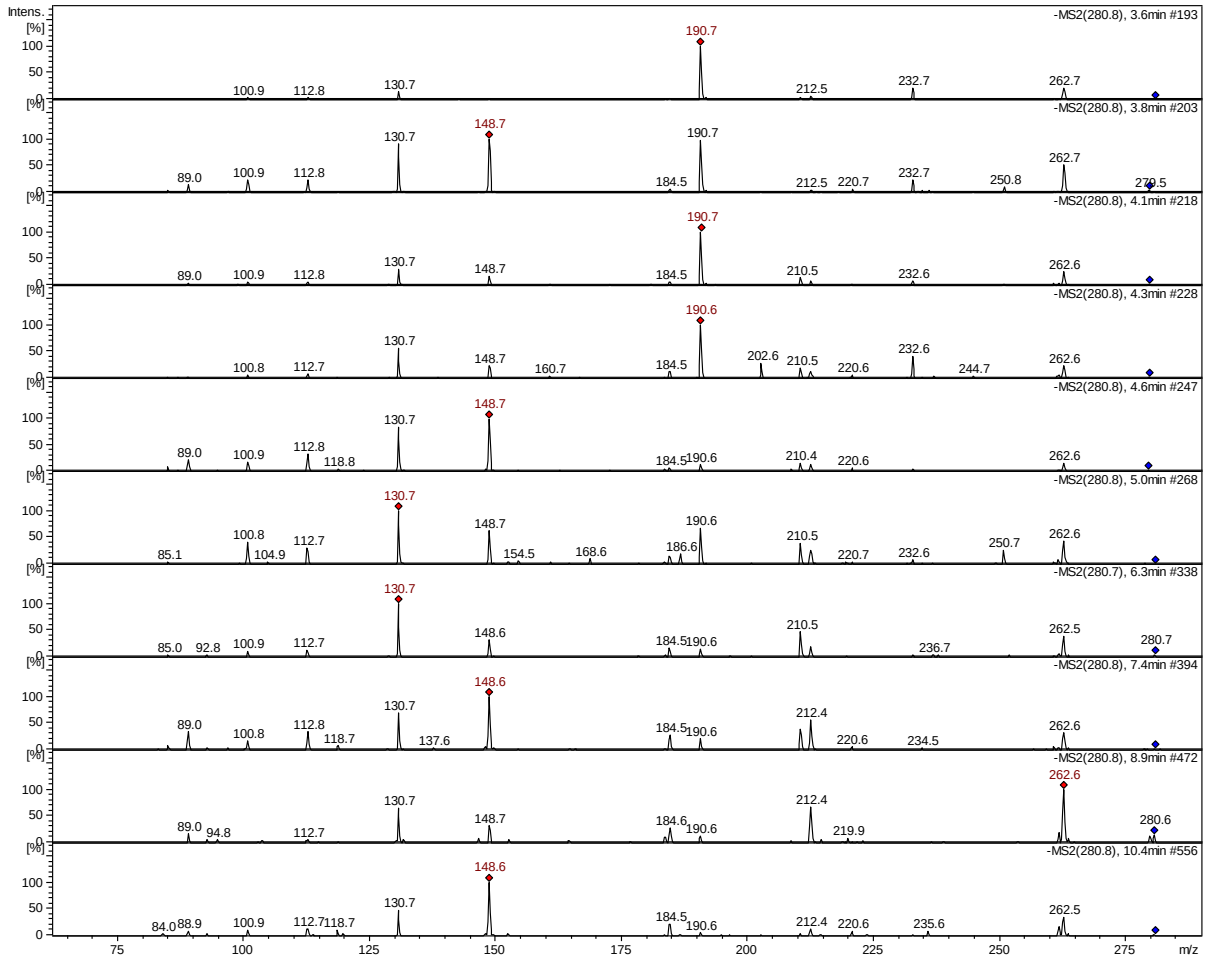

Figure S31 MS^2 spectra of fragment at *m/z* 281.0 ($C_{10}H_{18}O_9$) for ten chromatographic peaks of caramelised arabinose in the negative ion mode

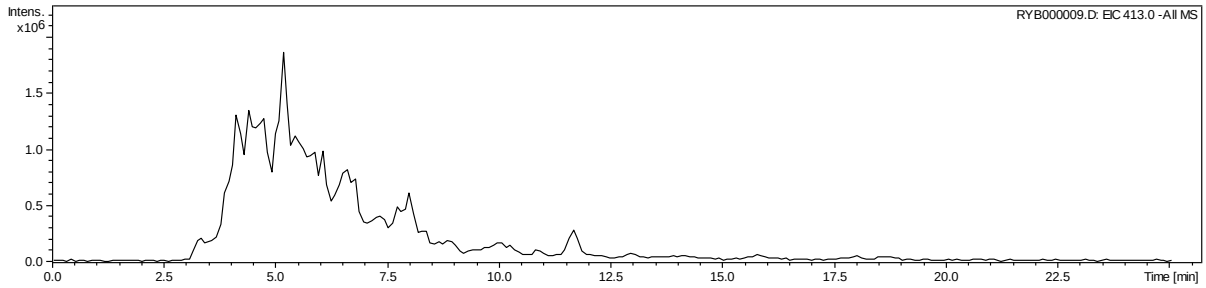

Figure S32 EIC at *m/z* 413.0 ($C_{15}H_{26}O_{13}$) for caramelised rybose in the negative ion mode

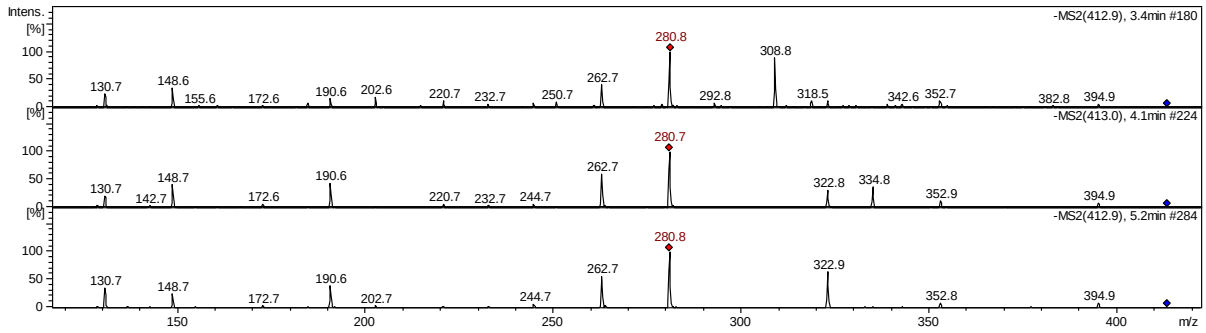

Figure S33 MS^2 spectra of fragment at *m/z* 413.0 ($C_{15}H_{26}O_{13}$) for three chromatographic peaks of caramelised rybose in the negative ion mode

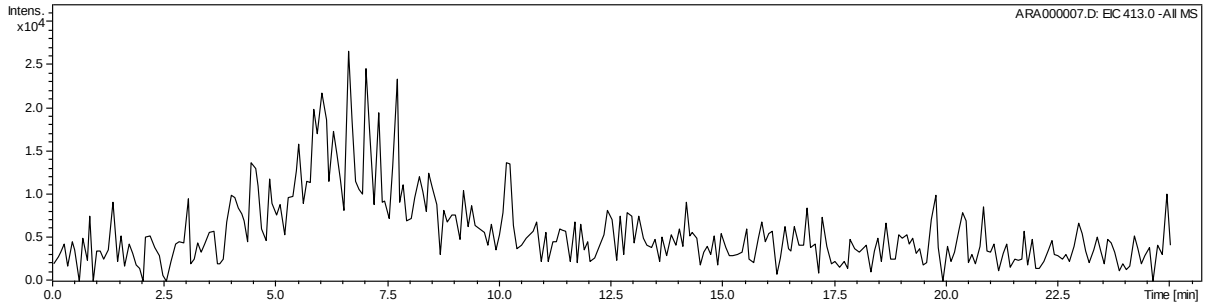

Figure S34 EIC at *m/z* 413.0 ($C_{15}H_{26}O_{13}$) for caramelised arabinose in the negative ion mode

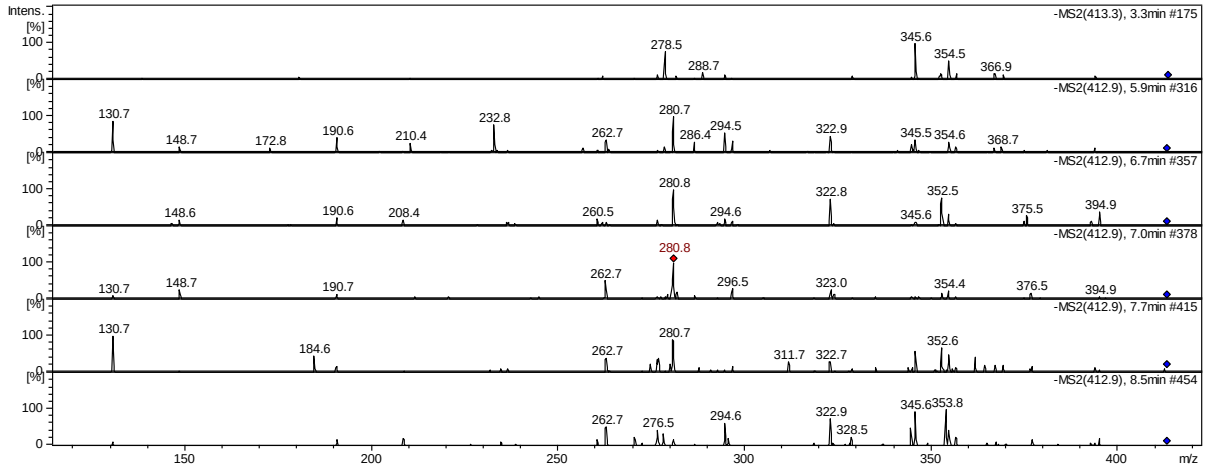

Figure S35 MS^2 spectra of fragment at *m/z* 413.0 ($C_{15}H_{26}O_{13}$) for six chromatographic peaks of caramelised arabinose in the negative ion mode

Dehydrated pentoses:

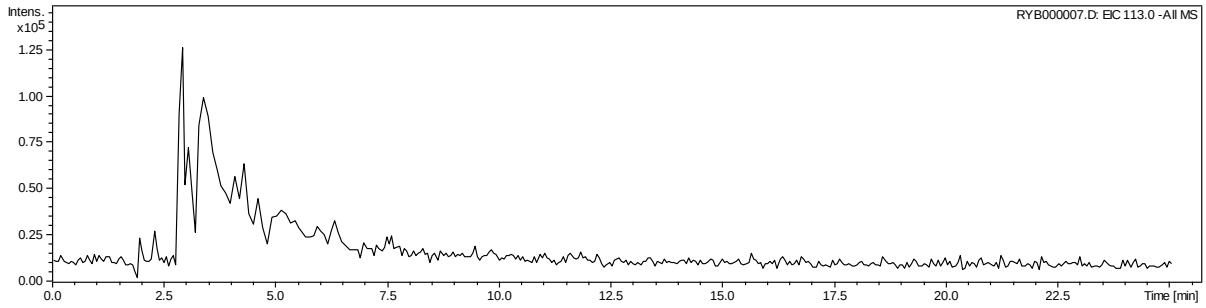

Figure S36 EIC at *m/z* 113.0 ($C_5H_6O_3$) for caramelised rybose in the negative ion mode

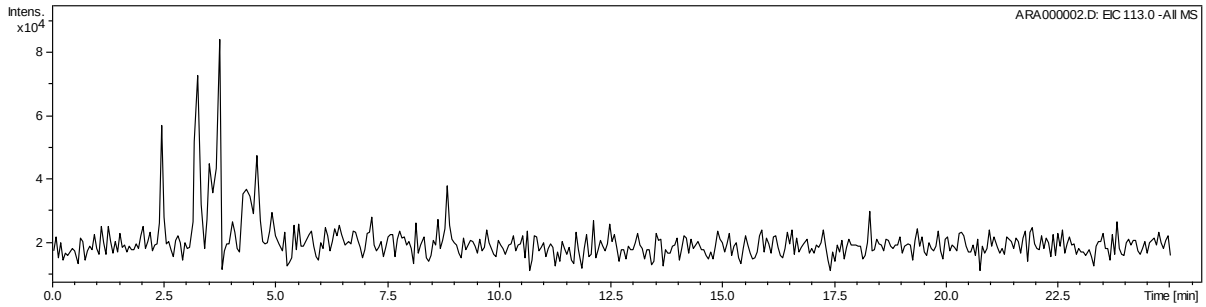

Figure S37 EIC at *m/z* 113.0 ($C_5H_6O_3$) for caramelised arabinose in the negative ion mode

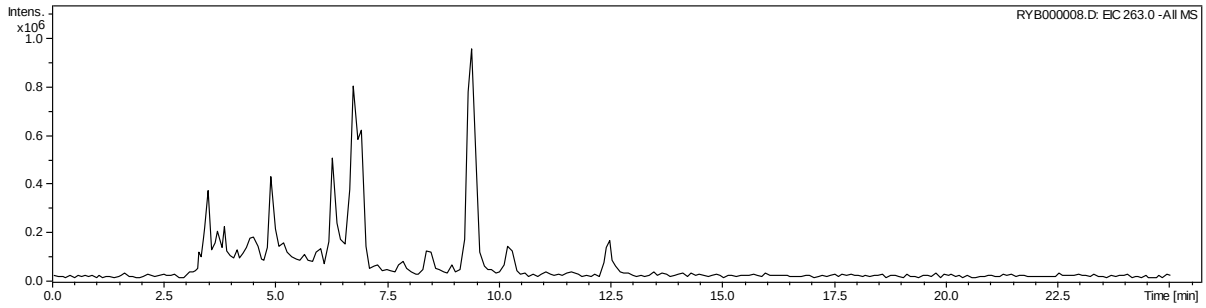

Figure S38 EIC at *m/z* 263.0 ($C_{10}H_{16}O_8$) for caramelised rybose in the negative ion mode

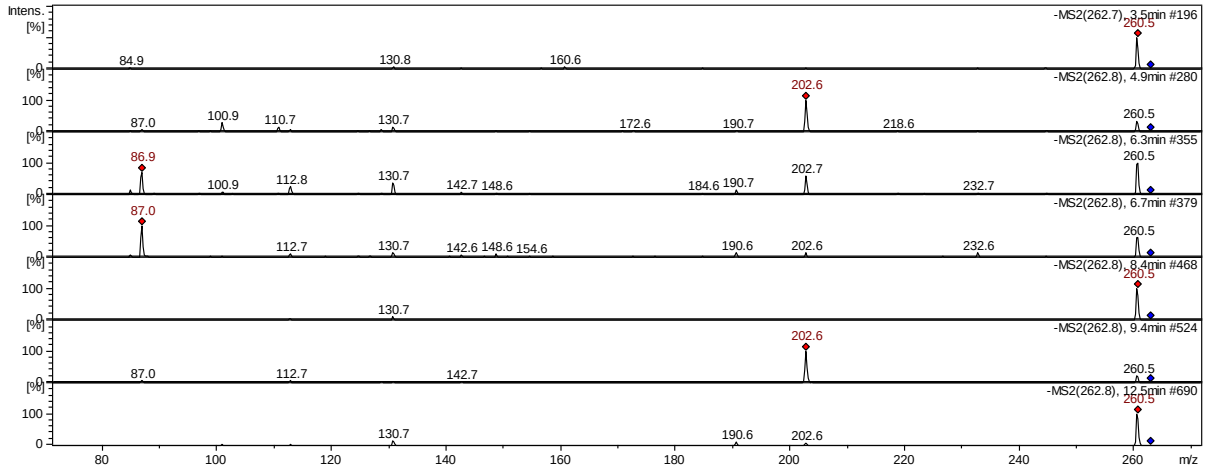

Figure S39 MS^2 spectra of fragment at *m/z* 263.0 ($C_{10}H_{16}O_8$) for seven chromatographic peaks of caramelised rybose in the negative ion mode

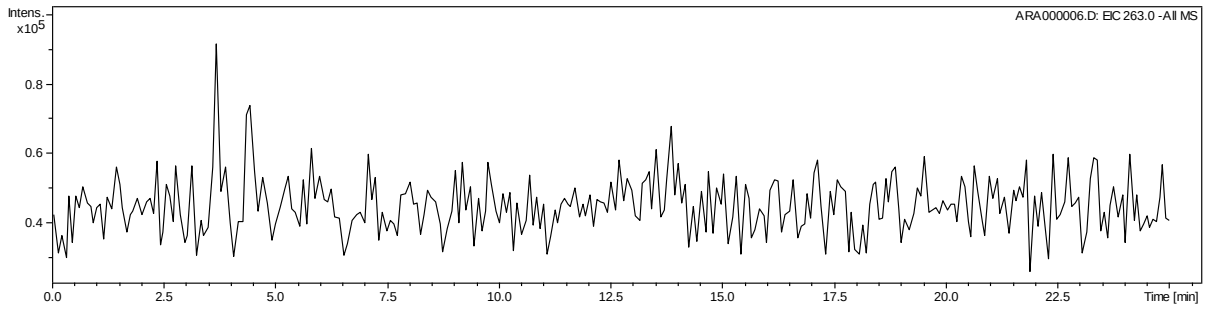

Figure S40 EIC at *m/z* 263.0 ($C_{10}H_{16}O_8$) for caramelised arabinose in the negative ion mode

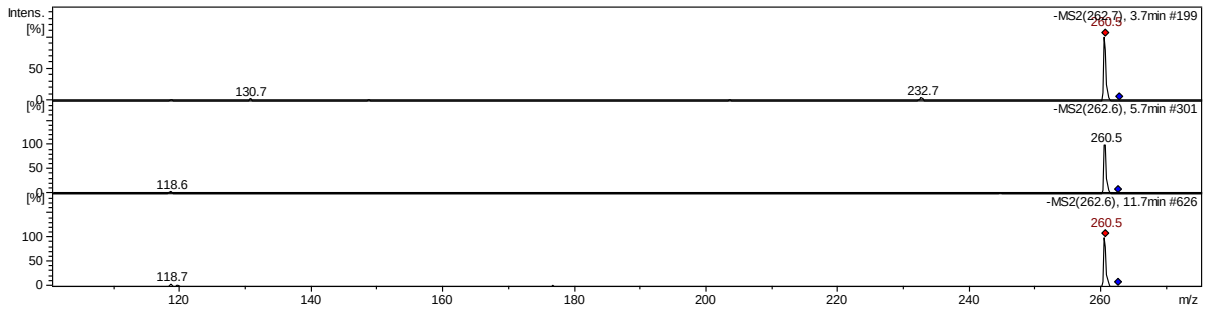

Figure S41 MS^2 spectra of fragment at *m/z* 263 ($C_{10}H_{16}O_8$) for three chromatographic peaks of caramelised arabinose in the negative ion mode

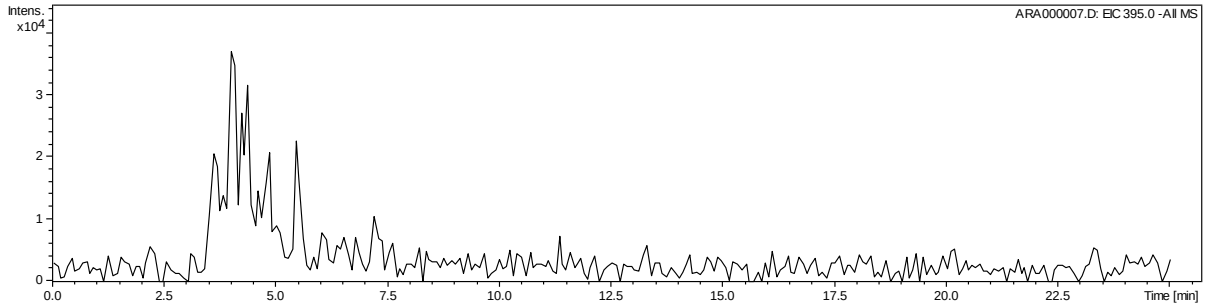

Figure S42 EIC at *m/z* 395.0 ($C_{15}H_{24}O_{12}$) for caramelised arabinose in the negative ion mode

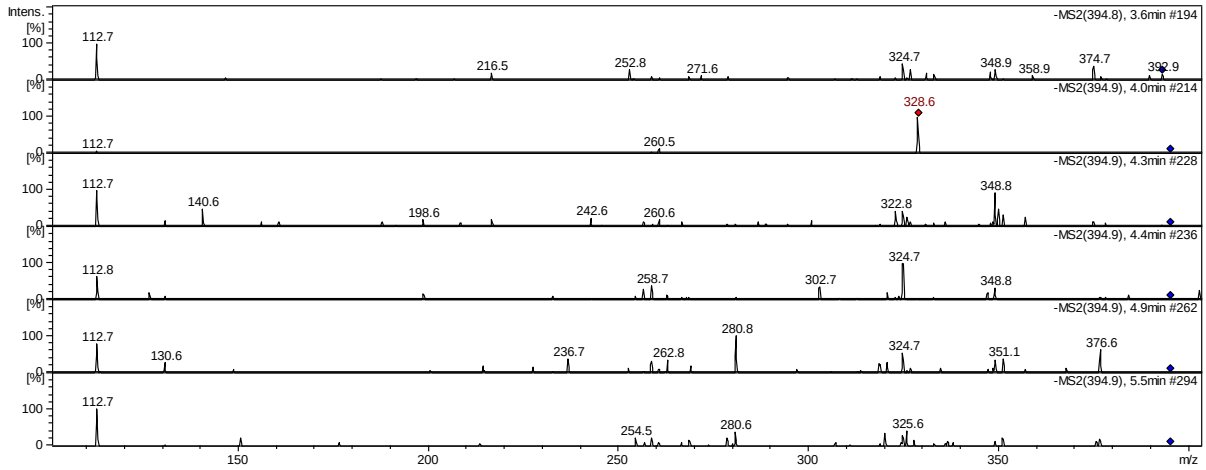

Figure S43 MS^2 spectra of fragment at *m/z* 395.0 ($C_{15}H_{24}O_{12}$) for six chromatographic peaks of caramelised arabinose in the negative ion mode

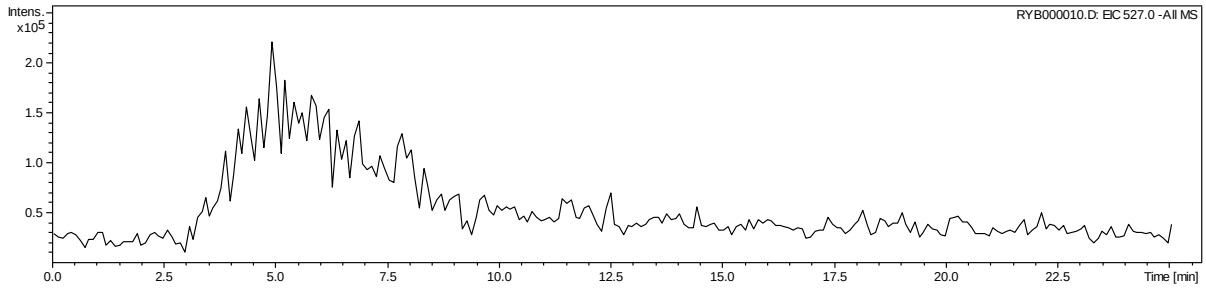

Figure S44 EIC at *m/z* 527.0 ($C_{20}H_{32}O_{16}$) for caramelised rybose in the negative ion mode

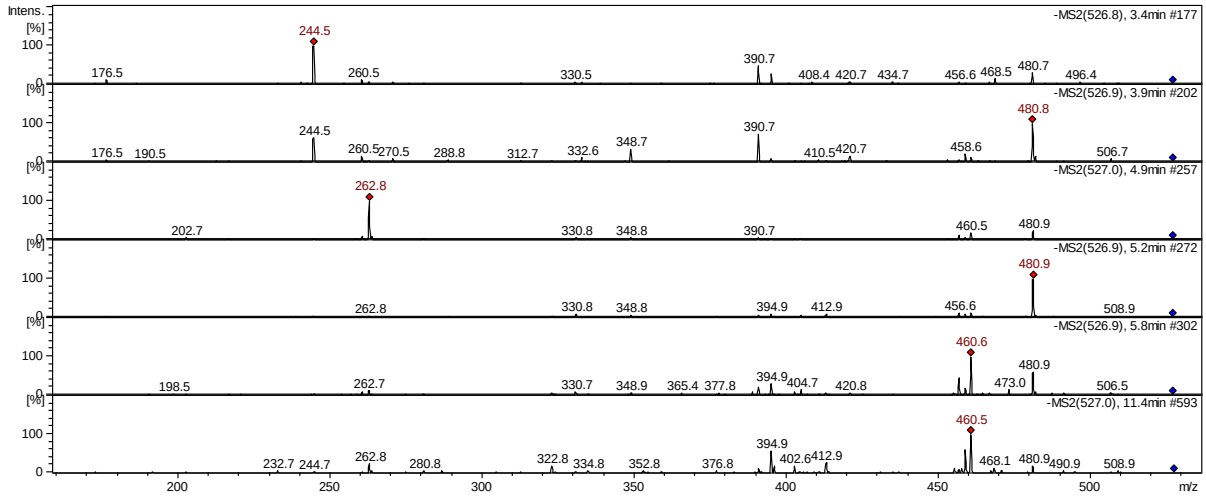

Figure S45 MS^2 spectra of fragment at *m/z* 527.0 ($C_{20}H_{32}O_{16}$) for six chromatographic peaks of caramelised rybose in the negative ion mode

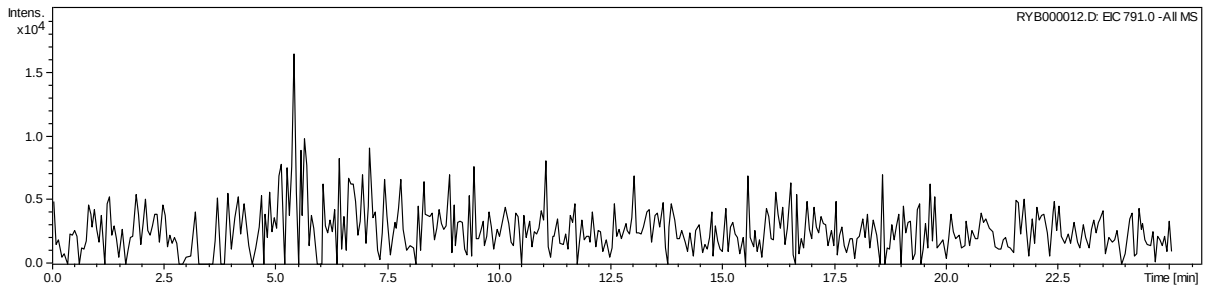

Figure S46 EIC at *m/z* 791.0 ($C_{30}H_{48}O_{24}$) for caramelised rybose in the negative ion mode

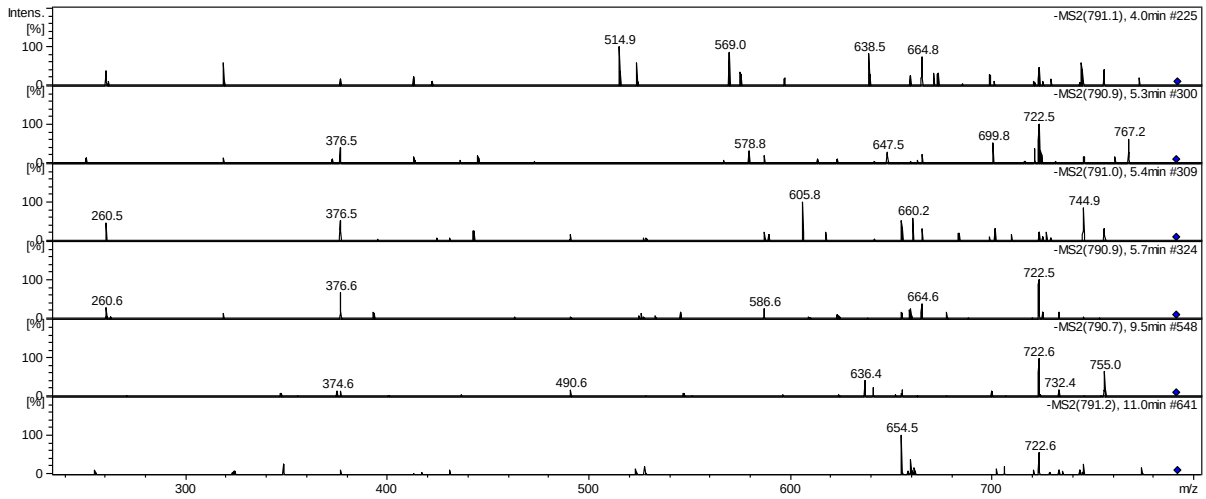

Figure S47 MS^2 spectra of fragment at *m/z* 791.0 ($C_{30}H_{48}O_{24}$) for six chromatographic peaks of caramelised rybose in the negative ion mode

Table S2 Negative ion mode ESI-MS/MS data for caramelised fructose

	MS^2	MS^3	MS^4
m/z	***m/z* (Intensity)**	***m/z* (Intensity)**	***m/z* (Intensity)**
160.8	113.1 (100.0); 101.2 (77.7); 131.0 (31.8); 71.6 (16.0); 83.4 (13.5)		
178.9	89.3 (100.0); 160.9 (98.5); 143.0 (85.2); 119.1 (67.6); 113.1 (34.8); 131.1 (30.5); 101.2 (24.9); 71.6 (17.4); 148.9 (16.9); 107.1 (13.4); 87.3 (13.0); 59.8 (10.1); 125.0 (9.0); 178.9 (3.4); 99.2 (2.2)	**142.9**: 125.0 (100.0); 87.3 (67.4); 115.1 (56.5) **89.2**: 71.6 (100.0); 59.8 (70.74) **119.0**: 101.2 (100.0); 89.3 (10.5) **131.0**: 113.1 (100.0); 101.2 (91.2)	
		160.8: 113.1 (100.0); 131.0 (47.4); 142.9 (32.8); 101.1 (14.3)	**113.0**: 95.2 (100) 85.4 (47.25)
283.1	264.9 (100.0); 217.9 (26.2); 114.1 (20.7); 283.1 (19.7); 246.8 (15.2); 221.9 (10.3); 186.9 (9.8); 220.8 (9.0)	**264.8**: 246.8 (100.0); 217.9 (57.01)	
322.9	160.9 (100.0); 232.9 (80.4); 113.1 (22.4); 322.9 (21.2); 143.0 (15.2); 178.8 (12.5); 202.9 (8.9); 274.9 (6.7); 101.2 (6.2); 304.9 (4.1); 131.0 (3.9); 250.9 (3.8); 220.9 (2.7); 119.1 (2.4); 292.9 (2.2); 125.1 (2.2)	**232.9**: 160.9 (100.0); 113.1 (67.6); 142.9 (65.2)	
341.0	178.9 (100.0); 322.9 (90.6); 160.9 (34.5); 220.9 (18.1); 341.0 (14.9)	**160.9**: 113.1 (100.0); 101.2 (50.4); 142.9 (47.7); 160.9 (25.3); 89.3 (22.1); 85.4 (16.5) **178.8:** 160.9 (100.0); 89.3 (88.6) **160.9**: 101.1 (100.0)	
367.0	276.9 (100.0); 186.9 (47.0); 348.9 (47.7); 204.9 (40.1); 367.0 (17.2); 168.9 (13.8); 330.9 (12.4); 127.0 (7.5); 156.9 (6.1); 306.9 (5.6); 192.9 (4.2); 190.9 (3.2); 336.9 (3.7); 178.9 (2.6); 172.9 (2.2); 113.1 (1.9); 125.1 (1.6); 258.8 (1.4); 312.9 (1.9); 216.8 (1.0)	**276.8**: 186.9 (100.0); 204.9 (93.9); 168.9 (38.6); 156.9 (14.6); 216.9 (6.9) **186.9**: 127.0 (100.0) **348.9**: 330.9 (100.0); 186.9 (78.3); 204.9 (73.2); 276.9 (26.6); 258.9 (33.6); 168.9 (40) **204.8**: 186.9 (98.7); 168.9 (100); 156.9 (44.4)	**186.9**: 115.1 (100.0) **204.9**: 168.9 (100.0)
413.2	344.9 (100.0); 252.9 (48.1); 322.9 (40.0)		
485.2	322.9 (100.0); 160.9 (19.3); 178.9 (9.2); 232.9 (7.9); 485.2 (7.2); 395.0 (5.6); 143.0 (3.9); 304.9 (3.7); 467.0 (2.7); 383.0 (2.6); 340.9 (1.4); 425.0 (1.1); 449.0 (1.1); 214.9 (1.0); 286.9 (0.9)	**322.9**:160.9 (100.0); 232.9 (87.2); 113.1 (27.0); 143.0 (13.9); 178.9 (10.3)	
503.2	340.9 (100.0); 485.0 (58.3); 413.0 (53.7); 178.9 (50.0); 322.9 (50.0); 383.0 (43.8); 160.9 (13.8); 250.8 (7.5); 443.0 (6.8); 220.8 (6.4)	**341**:178.9 (100.0)	
529.2	511.1 (100.0); 349.0 (60.1); 439.0 (33.6); 367.0 (20.2); 529.2 (17.0); 276.9 (16.6); 186.9 (12.8); 204.9 (11.4); 330.9 (4.9); 168.9 (3.7); 258.9 (3.3); 493.1 (3.2); 469.1 (2.2); 246.9	**511.1**: 348.9 (100.0); 439.0 (42.5); 168.8 (28.4); 276.9 (22.1); 258.9 (21.4); 168.9 (17.5)	

	(2.0); 481.1 (2.0)	**439.0**: 349.0(100.0) **349.0**: 186.8 (42.2); 258.9 (41.2)	
647.2	485.01 (100.0); 323.0 (34.4); 467.1 (3.6); 566.1 (2.4); 232.9 (1.7); 323.9 (1.4); 304.9 (1.3); 341.0 (1.1); 629.2 (0.9); 395.0 (0.8); 178.9 (0.6)	**485.1**: 322.9 (100.0); 232.9 (9.0)	**322.9**: 232.8 (67.3)
665.3	485.1 (100.0); 503.0 (87.0); 340.9 (70.9); 545.1 (52.3); 575.2 (49.2); 322.9 (38.9); 647.2 (36.3); 383.0 (34.5); 413.0 (26.9)		
683.2	647.2 (100.0); 485.1 (33.1); 503.0 (0.5)	**647.2:** 485.1 (100.0)	
691.2	511.1 (100.0); 673.2 (38.0); 348.9 (32.6); 439.0 (20.3); 529.1 (13.8); 601.2 (12.8); 691.2 (9.1); 367.0 (8.2)		
989.3	647.2 (100.0); 899.3 (55.6); 827.3 (47.8); 869.3 (42.3); 665.2 (42.2); 545.2 (38.7); 485.1 (29.0); 503.1 (21.0); 707.3 (20.2); 340.9 (18.6); 383.1 (17.4); 809.2 (16.6); 737.3 (16.1); 971.3 (16.0); 322.9 (11.2)		

Table S3 Negative ion mode ESI-MS/MS data for caramelised galactose

	MS^2	MS^3
m/z	***m/z* (Intensity)**	***m/z* (Intensity)**
160.9	113.1(100) 101.1 0(90.7) 131.0(47.8) 142.9(33.0) 89.2(13.9) 87.3(12.9)	
178.8	160.9(100) 89.3(61.5) 142.9(43.9) 119.0(35.7) 113.1(25.2) 131.0 (21.6) 101.2(21.6) 148.9(8.5) 87.3(7.6) 107.1(7.3) 125.0(6.2) 59.8(5.7) 71.5(5.5	**160.9:** 113.1 (100) 131.0 (68.82) 142.9(31.59)
220.9	160.9(100)	
255.0	236.9(100) 224.9(63.9) 75.4(60.8) 178.9(59.5)	
323.0	160.9(100) 113.1(34.9) 220.9(27.0) 232.8(26.8) 304.9(17.6) 178.9(17.2) 262.9(16.6) 142.9(15.2) 244.8 (6.4) 250.8 (6.0)	**161.0:** 113.1(100)
341.0	178.9(100) 322.9(69.3) 160.9(40.02) 250.9(30.2) 220.9(27.2) 142.9(22.4) 113.1(20.3) 119.0(14) 101.2 (13.3) 266.9 (11.2) 280.9(11.1) 125.0(8.5) 131.0(8.2) 311.0(7.8)	**179.0**: 89.3(100)
449.0	286.9(100) 431.0(65.8) 160.9(47.3) 322.9(33)	
485.2	322.9(100) 160.9(15.6) 178.9(6.4) 304.9(4.6) 467.1(4.2) 220.9(4.1) 383.0(3.2) 425.0 (3.0) 340.9(2.9) 449.1(2.8) 395.0 (2.5) 142.9(2.2) 364.9(2.0) 232.9(1.8) 262.9(1.8)	**323.0**: 160.9(100) 113.1(40.5) 232.9 (32.8)
503.0	340.9(100) 322.9(45) 383.0(29.5) 485.1(28) 178.9(27.2) 443.0(14.5) 220.9(13.2) 250.9(11.9) 413.0(11.9) 160.9(9.0) 280.9(6.6) 304.9 (6.0) 262.8(4.1)	**340.9**: 78.9(100)
		383.0: 220.9(100)
519.0	483.1(100)	
611.2	449.0(100) 431.0(18) 593.1 (17.9) 322.9(17.2) 286.9(15.5) 485.0 (8.8) 220.9(5.6) 521.1(4.3) 178.9(4.0)	
647.2	485.1(100) 323.0(32.4) 467.1(23) 566.2(4.6) 629.2(4.4) 304.9(3.3) 383.0(2.8) 341.0(2.8) 503.1(2.3) 220.9(2.1) 527.1(1.8) 611.2(1.6) 557.2(1.6) 365.0 (1.5) 587.2(1.4) 425.1(1.3) 545.2(1.3) 449.1(0.5) 262.9(0.5) 395.0(0.5) 250.9(1.1) 615.2(0.9) 244.9(0.8) 407.0(0.8) 232.9(0.7) 286.9(0.7) 393.0(0.7) 638.2(0.7) 362.9(0.6) 575.2(0.5) 413.1(0.5)	**485.1**: 322.9(100) 160.9(7.4) 220.9 (7.0) 304.9 (5.1)
665.2	503.1(100) 485.1(53.5) 647.2(44.5) 322.9(27.1) 383.0(26.7) 341.0(15.9) 545.2 (15) 443.1 (10.2) 220.9(7.0) 413.1(5.9) 605.2(5.6) 575.2 (4.4) 262.9(3.8) 280.9(3.8) 395.0 (3.3) 467.1(2.9) 629.2(2.8) 178.9(2.7) 664.3(2.6) 304.9(2.3) 160.9 (2) 425.1(1.8) 563.1(1.3)	**503.1**: 340.9(100) 322.9(38.4) 383.0(29.0) 178.9(18.8)
		485.1: 341.0 (70.43) 322.9(100)
		383.0: 220.9(100)
		545.2: 383.0(100)
683.2	647.2(100) 485.1(11.4) 665.2(10.9)	**647.2**: 485.1(100)
687.0	507.1(100) 525.1(68.5) 344.9(60.1) 363.0(52.1) 405.0 (46.2) 655.2 (41.1) 669.2 (28.4) 242.9(27.8) 567.1(26.1) 272.9(20)	**525.1**: 344.9(100)
737.3	656.2(100) 575.2(83.0) 719.2(41.0) 596.2(22)	
773.3	611.2(100) 449.1(35.9) 593.2(25.6) 755.3(23.6) 323.0(11.6) 485.1(9.5) 431.0(8.3) 383.0(6.3) 491.1(6.0)	**611.2**: 449.1(100)
791.3	629.3(100) 647.2(58.9) 773.3(4102) 467.1(30.7) 611.2 (26.8) 755.2(26.8) 322.9(25)	

809.3	647.3(100) 485.1(33.6) 629.2(23.3) 467.1(9.4) 323.0(8.9) 791.3(3.8) 728.3 (3.7) 383.0(3.5) 503.2(2.7) 665.2(2.6) 545.2(2.5) 527.2(2.5) 689.3(2.4) 304.9(1.7) 341.0(1.4) 707.2 (1.3)	**647.3**: 485.1(100) 467.1(22.6) 323.0(23.6)
		485.1: 322.9(100)
827.3	665.2(100) 647.2(40.1) 485.1(39.9) 503.1(39.3) 809.3(32.3) 340.9 (16.3) 383.0(16.1) 545.1(15.6) 707.3(120.6) 322.9(9.2) 767.2(5.9) 737.2(5.5) 443.1(4.3) 831.2(3.4) 262.8(3.3) 467.0(3.1)	
972.3	810.3(100) 648.2(25.82)	
989.3	827.3(100) 665.3(62.8) 809.3(47.5) 647.2(40.7) 503.1(21) 545.2(20.9) 971.3(18.5) 383.0(17.1) 485.0(16.8)	

Table S4 Negative ion mode ESI-MS/MS data for caramelised mannose

	MS^2	**MS^3**	**MS^4**
m/z	***m/z* (Intensity)**	***m/z* (Intensity)**	***m/z* (Intensity)**
161.0	101.1(100) 113.1(86.9) 85.3(68.0)		
178.9	160.9(100) 135.0 (85.4 119.0 (79.1) 89.3(78.2) 150.9(71.8) 122.0(69.4)		
253.2	114.1(100) 191.9(78.2) 113.1 (61.8)		
255.0	113.1(100)		
279.9	114.1(100) 113.1(58.6) 219.9(8.2) 221.9(5.7) 218.9(4.5) 262.9(3.7) 251.9(3.6) 178.8(3.3) 165.9(2.5)		
283.1	114.1(100) 217.9(69.7) 264.9(66.9) 221.8(38.9) 255.9(20.9)		
322.9	160.9(100) 114.1(41.4) 220.9(38.3) 276.0(15.0) 113.1(12.2) 304.9(10.8) 232.9(9.1)		
341.0	322.9(100) 114.1(96.9) 279.9(82.9) 276.0(75.3) 178.9(35.9) 264.9(13.3) 294.0(11.7) 341.0 (11.0) 280.9 (10.2) 160.9(9.0) 220.9 (5.9) 119.1(4.7) 217.9(4.6) 113.1 (3.9) 250.9 (3.1) 221.9(2.8) 282.9(2.6)	**323.0**: 275.9(85.05) 114.1 (100) 217.9(16.7)	**276.0**: 133(100)
		275.9: 232.9 217.9	
485.1	322.9(100) 178.9(9.7) 220.9 (9.3) 160.9(8.5) 341.0(7.4) 467.1(7.0) 425.0(4.8) 304.9(4.5)	**323.0**: 160.9(100)	
503.1	340.9(100) 443.1(73.6) 383.0(42.0) 485.1(40.1) 322.9(38.1) 178.9(36.9) 413.0(18.5) 220.9(12.3) 160.9(9.3) 280.9(8.1) 425.0(7.5) 304.9(7.2) 262.9(5.2) 250.9(4.7)	**341.0**: 178.9 (100)	
647.2	485.1(100) 322.9(21.0) 467.1 (15.7) 629.2 (10.0) 425.0(7.4)	**485.1**: 322.9(100)	
665.2	503.1(100) 647.2(45.5) 341.0(43.8) 485.1(41.8) 605.2(38.4) 545.1(35.1) 383.0(32.7) 443.1(23.9) 323.0(19.1) 575.2(15.6) 587.2(10.0) 413.0(9.9) 467.1(4.3) 280.9(4.0) 220.9(3.8) 304.9(3.1)		
691.2	673.2(100) 511.1(7.32) 348.9(3.43)	**673.2**: 511.1(100) 613.2(65.43) 655.2(32.4) 493.1(31.79)	

809.3	647.2(100) 629.2(27.7) 485.1(38.7) 791.3(13.4)		
827.3	665.2(100) 503.1(61.1) 647.2(37.0) 545.1(29.2) 707.2(27.4) 485.1(25.6) 809.3(22.8) 605.2(18.6) 383.0(15.2) 767.3(14.8) 341.0(12.2) 737.2(12.2) 443.1(11.4) 575.2(10)		
835.4	673.2(100) 775.3(83.5) 817.3(57.8) 511.1(43.1) 715.3(43.1) 493.1 (37.8) 745.3(35) 665.2(34.8) 451.1(21.3) 613.2(20.8) 553.1(16.2)		
989.4	827.3(100) 665.2(65.0) 503.1(37.3) 809.2(35.6) 647.2(34.0) 929.2(25.8) 707.2(22.7) 869.3(22.3) 485.0(20.4) 971.2 (20)		
1151.4	989.3(100) 827.3(62.21)		
1313.4	1151.3(100)		
1321.4	1159.3(100) 1261.4(54.96) 1303.4(59.80) 1201.3(33.08) 1141.4(42.75) 997.3(50.64) 835.3(38.93) 673.2(25.7)		